1 **Efficacy and limitations of senolysis in atherosclerosis**

2

3 Abel Martin Garrido[1], Anuradha Kaistha[1], Anna K Uryga[1], Sebnem Oc[1], Kirsty Foote[1], Aarti
4 Shah[1], Alison Finigan[1], Nichola Figg[1], Lina Dobnikar[1,2], Helle Jørgensen[1], Martin Bennett[1,*]

5

6 [1]Division of Cardiovascular Medicine, University of Cambridge, and [2]Nuclear Dynamics
7 Programme, Babraham Institute, Cambridge UK

8

9 **Short title:** Senolysis in atherosclerosis

10

11 Abel Martin Garrido and Anuradha Kaistha contributed equally to this paper.

12

13 ***Correspondence**
14 Division of Cardiovascular Medicine,
15 University of Cambridge,
16 Box 110, ACCI,
17 Addenbrooke's Hospital,
18 Cambridge, CB2 2QQ, UK
19 Email:mrb24@medschl.cam.ac.uk
20 Telephone: 01223 331504

Word Count 8735
Figures 6
Tables 0

21
22 **Original Article**
23
24
25
26
27

1 **Abstract**
2 **Aims**: Traditional markers of cell senescence including p16, Lamin B1, and senescence-
3 associated beta galactosidase (SAβG) suggest very high frequencies of senescent cells in
4 atherosclerosis, while their removal via 'senolysis' has been reported to reduce atherogenesis.
5 However, selective killing of a variety of different cell types can exacerbate atherosclerosis.
6 We therefore examined the specificity of senescence markers in vascular smooth muscle cells
7 (VSMCs) and the effects of genetic or pharmacological senolysis in atherosclerosis.
8
9 **Methods and Results:** We examined traditional senescence markers in human and mouse
10 VSMCs *in vitro*, and in mouse atherosclerosis. p16 and SAβG increased and Lamin B1
11 decreased in replicative senescence (RS) and stress-induced premature senescence (SIPS)
12 of cultured human VSMCs. In contrast, mouse VSMCs undergoing SIPS showed only modest
13 p16 upregulation, and proliferating mouse monocyte/macrophages also expressed p16 and
14 SAβG. Single cell RNA-sequencing (scRNA-seq) of lineage-traced mice showed increased
15 p16 expression in VSMC-derived cells in plaques *vs.* normal arteries, but p16 localized to
16 Stem cell antigen-1 (Sca1)$^+$ or macrophage-like populations. Activation of a p16-driven suicide
17 gene to remove p16$^+$ vessel wall- and/or bone marrow-derived cells increased apoptotic cells,
18 but also induced inflammation and did not change plaque size or composition. In contrast, the
19 senolytic ABT-263 selectively reduced senescent VSMCs in culture, and markedly reduced
20 atherogenesis. However, ABT-263 did not reduce senescence markers *in vivo*, and
21 significantly reduced monocyte and platelet counts and IL6 as a marker of systemic
22 inflammation.
23
24 **Conclusions:** We show that genetic and pharmacological senolysis have variable effects on
25 atherosclerosis, and may promote inflammation and non-specific effects respectively. In
26 addition, traditional markers of cell senescence such as p16 have significant limitations to
27 identify and remove senescent cells in atherosclerosis, suggesting that senescence studies in
28 atherosclerosis and new senolytic drugs require more specific and lineage-restricted markers
29 before ascribing their effects entirely to senolysis.
30

31 **Translational Perspective**
32 Senescent vascular smooth muscle cells promote atherogenesis and features of plaque
33 instability, suggesting that clearance of senescent cells (Senolysis) may represent a novel
34 therapeutic strategy. However, we find that traditional senescence markers are not specific in
35 atherosclerosis, and p16-based senolysis promotes inflammation without changing
36 atherosclerosis extent or architecture. The senolytic ABT-263 selectively kills senescent
37 smooth muscle cells and reduces atherosclerosis, but also reduces blood counts, which may
38 partly underlie its anti-atherosclerosis effect. Our studies highlight both limited efficacy and
39 non-specific effects of senolysis in atherosclerosis*,* and limitations of conventional markers to
40 identify and remove senescent cells.
41
42
43

1 **1. Introduction**
2 Cell senescence is defined by the (normally) irreversible proliferative arrest of cells that can
3 usually divide. Senescence is induced by exhaustion of replicative potential, for example by
4 telomere shortening, or as a stress response, the so-called 'stress-induced premature
5 senescence' (SIPS). Both replicative senescence (RS) and SIPS are characterized by cell
6 cycle withdrawal, expression of 'markers' (including cyclin-dependent kinase inhibitor p16^{ink4a}
7 (p16) and senescence-associated beta galactosidase' (SAβG) enzyme activity), and secretion
8 of a cytokine panel (the 'senescence-associated secretory phenotype' (SASP)).
9
10 Senescent cells have been identified in atherosclerosis, particularly endothelial and vascular
11 smooth muscle cells (VSMCs)(reviewed in[1]). Reported evidence includes p16 expression,
12 telomere shortening compared with normal arteries, and SAβG activity[2]. However,
13 identification of senescent cells *in vivo* in a heterogeneous atherosclerotic plaque is
14 problematic. For example, although the fibrous cap contains infrequent intensely SAβG-
15 positive cells that also express p16, most SAβG-positive cells in human lesions are in the
16 lesion core[2,3]. Similarly, the 'canonical' SASP markers such as matrix metalloproteinases
17 (MMPs), tumour necrosis factor alpha (TNFα), IL6 and IL1α can be expressed by
18 macrophages or other leukocytes, particularly after activation or DNA damage[4].
19
20 Studies using p16-directed cell suicide genes[5] or transgenic expression of telomere protein
21 mutants[6] or progerin[7] have suggested that cell senescence promotes plaque formation,
22 accelerates established lesions, and changes plaque composition, leading to increased
23 necrotic cores and smaller fibrous caps. However, recent studies have found that p16-
24 expressing murine mesenchymal cells are not necessarily senescent[8], that p16 and SAβG
25 can be expressed by mouse macrophages in response to immune stimuli[9], deletion of p16$^+$
26 cells *in vivo* can have neutral or detrimental effects[10,11], and some drug combinations to
27 remove senescent cells (senolytics) have no effect on atherosclerotic plaque development or
28 composition[12]. Any anti-atherosclerotic effects of deleting senescent cells could also be offset
29 by pro-atherosclerotic effects of inducing apoptosis in VSMCs and macrophages in
30 plaques[1,13]. We therefore examined the specificity and expression of traditional markers of cell
31 senescence in human and mouse VSMCs in culture and in mouse atherosclerosis, and the
32 effects of senolysis through activation of a p16-driven suicide gene or the senolytic drug ABT-
33 263.
34

1
2 **2. Methods**
3 The data underlying this article will be shared on reasonable request to the corresponding
4 author.
5
6 **2.1 Isolation of human VSMCs**
7 Human tissue was obtained under written informed consent using protocols approved by the
8 Cambridge or Huntingdon Research Ethical Committee and conformed to the principles
9 outlined in the Declaration of Helsinki. Primary human aortic VSMCs were isolated from medial
10 tissue explants as described in **Supplementary Material** online.
11
12 **2.2. Isolation of mouse VSMCs**
13 All animal experiments were regulated under the Animals (Scientific Procedures) Act 1986
14 Amendment Regulations 2012 following ethical review by Cambridge University Animal
15 Welfare and Ethical Review Body (AWERB). Mice were anaesthetized when necessary with
16 2.5% inhalable isofluorane (maintained at 1.5%), monitoring respiratory and heart rates,
17 muscle tone and reflexes. Mice were euthanised by CO_2 overdose. p16-3MR mouse aortic
18 VSMCs (mVSMCs) were isolated by enzymatic digestion as described in **Supplementary**
19 **Material** online**.**
20
21 **2.3. Isolation of mouse bone marrow-derived macrophages**
22 Mouse bone marrow-derived macrophages (BMDM) were isolated, cultured and differentiated
23 as described in **Supplementary Material** online.
24
25 **2.4. qPCR**
26 mRNA was isolated using Nuceolspin RNA columns (Macherey-Nagel, Düren, Germany).
27 cDNA was synthesized using a Quantitect Reverse Transcription Kit (Qiagen, UK) or
28 Omniscript RT Kit (Qiagen, UK) and 6ng or 7.5ng cDNA was used for quantitative PCR
29 (qPCR). qPCR conditions and quantification were as described in **Supplementary Material**
30 online.
31
32 **2.5. EdU incorporation**
33 Cells were incubated with 5-ethynyl-2'-deoxyuridine (EdU) for 24h and assayed using the
34 Click-iT^TM Plus EdU Cell Proliferation Kit for Imaging, Alexa Fluor^TM 647 dye (ThermoFisher
35 Scientific, MA, USA) as described in **Supplementary Material** online.
36
37 **2.6. SAβG activity**
38 SAβG activity *in vitro* was assayed using the Senescence Cells Histochemical Staining Kit
39 (Merck KGaA, Darmstadt, Germany) following the manufacturer's recommendations as
40 described in **Supplementary Material** online.
41
42 **2.7. Western blots**
43 Cells were lysed using RIPA buffer supplemented with a Protease Cocktail Inhibitor Set III
44 (Merck KGaA, Darmstadt, Germany), sonicated on ice for 10s, and protein concentration
45 determined from a standard curve either using a Bradford assay (Bio-Rad Laboratories Inc,
46 CA, USA) or Pierce BCA protein assay kit (Thermo Fisher Scientific Ma, USA). Lysates were
47 mixed with Laemmli buffer using β-mercapto-ethanol as a reducing agent, boiled at 98°C for
48 7 min, and stored at -80°C or lysates were mixed with LDS (4x) and reducing agent (10x) and
49 boiled at 95°C for 5 min. Protein separation, transfer and detection were as described in
50 **Supplementary Material** online.
51
52 **2.8. Confocal microscopy of human plaques**
53 Formalin-fixed paraffin-embedded human carotid endarterectomy sections were
54 permeabilised with 0.1% triton X-100 for 10 min, washed 3 times for 5 min before blocking
55 with 10% goat serum (DAKO X0907) for 1h at room temperature. Sections were incubated

1 with either primary antibodies: p16 (20µg rabbit polyclonal, ProSci 4211), Smooth muscle cell
2 α-actin-cy[3]-conjugated (1:1000 mouse monoclonal, Sigma-Aldrich C6198), CD68 (1:100
3 mouse monoclonal, Thermo 14-0689-82) or isotype control antibodies: rabbit monoclonal IgG
4 isotype control (Abcam ab172730), mouse monoclonal IgG isotype control (Abcam ab37355)
5 diluted in 3% BSA for 1h at room temperature. After washing 3 times for 5 min at room
6 temperature, sections were incubated with secondary antibodies: goat anti-rabbit Alexa Fluor
7 647 (1:500, Abcam ab150083) or goat anti-mouse Alexa Fluor 488 (1:800, Invitrogen A-
8 11017) for 1h at room temperature. After counterstaining with DAPI for 10 min at room
9 temperature and 3X washing for 5 min, sections were mounted in ProLong Gold antifade
10 mountant (Invitrogen P36930). Four different symptomatic human carotid artery sections were
11 analysed.
12
13 **2.9. Single cell RNA-sequencing**
14 Single cell RNA-sequencing (scRNA-seq) profiles are from animals where VSMC lineage-
15 tracing is achieved using the Myh11-cre[ERT2]/Rosa 26-Confetti system (Gene Expression
16 Omnibus accession number GSE117963)[14]. Datasets from enzyme-dispersed whole normal
17 aorta of ApoE^{+/+} or confetti[+] VSMCs from atherosclerotic fat-fed ApoE^{-/-} animals (plaques +
18 medial cells) were analysed using CRAN R package Seurat v.3.1.2 (PMID: 29608179; PMID:
19 31178118) in R v.3.6.2. The datasets were filtered for low quality cells as described[14] and
20 normalized using SCTransform (PMID: 31870423) v.0.2.1 for dimension reduction and
21 clustering steps. Highly-variable genes (3,000) were used in the calculation of principal
22 components (PCs). The first 30 (plaque) and 29 (whole aorta) PCs were used for Uniform
23 Manifold Approximation and Projection (UMAP) and clustering. Clustering was performed with
24 resolution 1.1 (plaque) and 0.7 (whole aorta).
25
26 **2.10. p16-3MR mouse experiments**
27 Male and female C56BL/6J ApoE^{-/-} mice were combined in all groups and used for all
28 experiments, either alone or fully backcrossed (>5x) with C56BL/6J/p16-3MR mice.
29 Genotyping of p16-3MR and ApoE^{-/-} mice was as described as described in **Supplementary**
30 **Material** online as described previously[15]. For bone marrow reconstitution, p16-3MR/ApoE^{-/-}
31 homozygous mice received 9Gy total body irradiation and 12x10^{6} bone marrow cells in 200µL
32 of PBS injected through the tail vein. 4 weeks later, gDNA was isolated from blood and p16-
33 3MR assayed compared with donor gDNA to quantify bone marrow reconstitution.
34
35 We studied atherogenesis in five experimental ApoE^{-/-} mouse groups receiving irradiation and
36 bone marrow transplant: ApoE^{-/-}→ ApoE^{-/-}, p16-3MR/ApoE^{-/-}→ ApoE^{-/-}, ApoE^{-/-}→ p16-3MR/
37 ApoE^{-/-}, p16-3MR/ApoE^{-/-}→ p16-3MR/ApoE^{-/-} mice + ganciclovir (GCV), or p16-3MR/ApoE^{-/-}
38 → p16-3MR/ApoE^{-/-} mice + saline. Mice were weaned at 3w of age, and fed on high fat
39 (Western) diet at 8w of age. 5mg/kg GCV in PBS or PBS control was administered
40 intraperitoneally once daily for 5 days, followed by 14 days without treatment on a repeating
41 cycle for the study duration.
42
43 **2.11. Bioluminescence *in vivo* imaging**
44 Mice were injected with 150µL of RediJect Coelenterazine H Bioluminescent Substrate
45 (150µg/mL, Perkin Elmer) intraperitoneally and luminescence was detected using a NightOWL
46 as described in **Supplementary Material** online.
47
48 **2.12. Oil-Red-O analysis of atherosclerosis**
49 Descending aortas were dissected and fixed overnight in 4% formaldehyde at 4°C. Aortas
50 were washed three times in PBS, adventitia removed under a dissecting microscope, opened
51 to expose the lumen, and incubated for 2 min in 60% isopropanol, followed by 10 min in Oil-
52 Red O staining solution (0.2g/ml Oil-Red O (Merck KGaA, Darmstadt, Germany) dissolved in
53 isopropanol and filtered). Aortas were washed again in 60% isopropanol for 2 min, transferred
54 to a microscope slide (Thermo Fisher Scientific Ma, USA) and coverslipped. Images were

1 taken at 4X magnification using Image Pro-Insight 9.1 (Media Cybernetics, MD, USA)
2 software, and total plaque area analysed using ImageJ (NIH, MD, USA).
3
4 **2.13. Aortic plaque quantification**
5 Aortic root sections were stained with Masson's trichrome and 4X images were captured using
6 a bright-field microscope with Image-Pro Insight 9.1 (Media Cybernetics, MD,
7 USA). Crystalline clefts between collagen fibres were used to identify plaques. The
8 boundaries of lumen and outer wall were outlined and areas of fibrous cap (rich in SMC
9 and extracellular matrix) and necrotic core (rich in cholesterol and cellular debris) were
10 identified and quantified using ImageJ software. TUNEL and Mac-3 immunohistochemistry
11 were performed as described in **Supplementary Material** online.
12
13 **2.14. Lipids, cytokines, blood counts**
14 Cytokine concentrations in mouse serum were measured using V-PLEX Mouse
15 Proinflammatory Panel 1 and U-PLEX Chemokine Combo immunoassays (Meso Scale
16 Discovery, MD, USA) following the manufacturer's recommendations. Serum lipids were
17 analyzed using Siemens Dimension EXL analyzer, and high-density lipoproteins (HDL)
18 analyzed using a Siemens Dimension RxL analyzer. Low-density lipoprotein (LDL)
19 concentration was calculated from the triglyceride, HDL and cholesterol concentrations using
20 the Friedwald formula (LDL = Cholesterol - HDL - (Triglycerides/2.2). Blood was taken from
21 experimental animals at beginning and end of the each dosage cycle and blood counts
22 analyzed on a Coulter counter. Blood pressures were determined using the tail cuff method.
23
24 **2.15. ABT-263 experiments**
25 ApoE$^{-/-}$ mice were weaned at 3w, and fed a high fat (Western diet) at 8w. Mice were
26 administered vehicle (ethanol/polyethylene glycol 400 (Sigma, MO, USA)/Phosal 50PG
27 (Lipoid GmbH, Ludwigshafen, Germany) at 10:30:60, or ABT-263 (Active Biochem, Kowloon,
28 HK) at 50mg/kg/day for 5 days for 3 cycles by gavage[16,17], each cycle separated by 3 weeks.
29
30 **2.16. Statistics**
31 Shapiro–Wilk test was used to determine if a dataset followed a normal distribution. Statistical
32 significance was determined by one-way ANOVA for normally distributed data followed by
33 Tukey's or Bonnferroni's multiple comparison test when more than 2 groups were compared.
34 Kruskal-Wallis H Test with Dunn's multiple comparisons test correction were used when more
35 than 2 groups were compared when data were not normally distributed. Unpaired Students t-
36 tests were used for comparing two groups which were normally distributed with similar SDs,
37 or Welch's t-test without similar SDs. Mann Whitney U test was used for two groups which
38 were not normally distributed. Data are expressed as mean, error bars represent SD and
39 $p < 0.05$ considered statistically significant.
40

1 **3. Results**
2
3 **3.1. Expression of senescence markers in human VSMCs in culture**
4 To examine expression of senescence markers in human VSMCs, we first established robust
5 cell culture models of SIPS and RS. In replicating control samples, 64% of cells incorporated
6 EdU over 24h and 12% were SAβG⁺. Samples reaching RS, defined as unchanged cell
7 number over a 14 day period, showed 8.3% EdU⁺ and 74% SAβG⁺ cells. To model SIPS, cells
8 were treated with 500nM doxorubicin for 1d and then allowed to recover for 21d (Dox 1d +
9 21d), where they showed 5.5% EdU⁺ and 86% SAβG⁺ cells compared with 34% EdU⁺, 23%
10 SAβG⁺ in control replicating cells from the same isolate sub-cultured for 21d (Control
11 1+21d)**(Figure 1A)**. Replicating (Control) cells expressed Lamin B1, but expression was
12 reduced 24h after Doxorubicin (Dox 1d), and by both SIPS (Dox 1d + 21d) and RS **(Figure
13 1B)**. Replicating cells had low p16 mRNA expression, p16 increased 2-fold with ongoing
14 culture (Control 21d), and ~4-fold by SIPS and RS **(Figure 1C)**. p16 and Lamin B1 were not
15 just marking DNA damage, as p21 was increased by Dox 1d, but not increased by RS **(Figure
16 1D)**. Lamin B1, p16, and p21 protein expression were similar to mRNAs, while both p21 and
17 p53 were increased by Dox 1d but not by RS or SIPS **(Figure 1E)**, indicating that both p53
18 and its target p21 are markers of predominantly DNA damage in human VSMCs, and not
19 senescence.
20
21 **3.2. p16 and Lamin B1 expression show a negative correlation in human VSMCs in**
22 **culture**
23 Lamin B1 and p16 appear reliable markers of human VSMC senescence *in vitro*; however,
24 their kinetics were unclear, particularly whether they mark pre-senescent cells (where
25 replication is still occurring), or are restricted to established senescence with irreversible
26 replication arrest. Primary human VSMC cultures showed marked heterogeneity of lifespan
27 with RS between passage (p) 5-15; however, p16 and Lamin B1 protein expression appeared
28 to be inversely correlated in individual primary cultures **(Supplementary Material** online,
29 *Figure S1A,B*). p16 mRNA levels showed a gradual increase with increasing passage number
30 and reduced proliferation at pre-senescence (p8-9), but with no further increase at
31 senescence (p11-15)**(Supplementary Material** online, *Figure S1C*); in contrast, Lamin B1
32 mRNA expression was maintained at pre-senescence but markedly reduced by established
33 senescence **(Supplementary Material** online, *Figure S1C*), suggesting that p16 expression
34 can trigger senescence and loss of Lamin B1. Similarly, using EdU labelling of proliferating
35 cells and immunocytochemistry, the percentage of p16⁺ cells increased at pre-senescence
36 with no further increases with established senescence (**Supplementary Material** online,
37 *Figure S1D,E*). Thus, human VSMCs undergoing senescence show reduced %EDU⁺,
38 increased %SAβG⁺, increased p16, and reduced Lamin B1 expression; however, p16
39 expression increases at a pre-senescent stage, but overall increased ≤4-fold compared with
40 replicating cells in both RS and SIPS.
41
42 **3.3. Mouse VSMCs express p16, p21, SAβG activity and p16-directed transgenes in**
43 **culture, but this is not associated with cell senescence**
44 Expression of p16 and p16 promoter-driven transgenes have been used to identify and
45 remove senescent cells in mouse models of vascular disease[2,5,18], although in some cases
46 the identity of the p16⁺ cell was not identified. To examine whether p16, Lamin B1 and p16
47 promoter activity can be used to identify senescent mouse VSMCs, we cultured VSMCs from
48 p16-3MR mice, which express a trimodal reporter construct encoding *Renilla* luciferase,
49 monomeric red fluorescent protein (RFP) and herpes simplex virus thymidine kinase (TK) from
50 a modified p16 promoter[16,19]. TK converts ganciclovir (GCV) into a toxic DNA chain terminator
51 to selectively kill HSV-TK–expressing cells. Upon senescence, cells from p16-3MR animals
52 can be marked by luciferase, sorted by RFP, and killed by GCV, providing a system also for
53 selective removal of senescent cells *in vivo*[16,19], including in arteries[5].
54

1 RS is difficult to achieve in mouse VSMCs in culture, as growth arrest is followed by crisis and
2 the culture re-established by faster replicating cells; SIPS was therefore induced in primary
3 mouse VSMCs by treatment with increasing Dox concentrations for 24h, followed by 7 days
4 recovery (Dox 1+ 7d). Dox treatment dose-dependently reduced %EdU$^+$ and Lamin B1
5 expression, and increased %SAβG$^+$ and the SASP marker IL6, consistent with SIPS (*Figure*
6 *1F-I*), **Supplementary Material** online, *Figure S2*). p16 and p21 mRNA expression increased
7 with SIPS, but by <2-fold for p16 and 4-fold for p21 (*Figure 1J-K*); again, apart from p21, the
8 pattern of protein expression generally followed mRNA expression, and was related to Dox
9 concentration (*Figure 1L*). We also analyzed expression of the p16-3MR reporter transgenes
10 luciferase and RFP and the response to GCV. Both mRNAs were detectable after SIPS of
11 mouse VSMCs (**Supplementary Material** online, *Figure S2*), and although there was no
12 relationship with %EdU$^+$ cells or Dox concentrations, p16-3MR/ApoE$^{-/-}$ VSMCs were
13 susceptible to killing by 10μg/ml GCV whereas ApoE$^{-/-}$ VSMCs were not (**Supplementary**
14 **Material** online, *Figure S3*). Furthermore, low-dose GCV did not reduce cell proliferation, but
15 selectively reduced SAβG$^+$ senescent vs. proliferating p16-3MR VSMCs (**Supplementary**
16 **Material** online, *Figure S4*). Thus, although mouse p16-3MR VSMCs show only a modest
17 increase in p16 mRNA expression on SIPS (<2-fold), and an inconsistent relationship between
18 expression of p16 and p16-directed reporters and cell senescence in culture, GCV selectively
19 kills senescent vs. proliferating p16-3MR VSMCs.
20
21 **3.4. Mouse macrophages express SAβG activity, p16, p16-directed reporter genes and**
22 **p21 upon differentiation in culture**
23 Macrophages in atherosclerosis arise from both migration from the bone marrow via peripheral
24 blood and proliferation of resident macrophages[20]. In addition, previous studies demonstrated
25 that foam cells expressing p16-3MR can be removed from atherosclerotic plaques by GCV[5].
26 We therefore isolated bone marrow-derived macrophages (BMDMs) from p16-3MR mice and
27 cultured them for 1d, 7d, 21d or 28d to allow differentiation. At 7d, 99% of the cells expressed
28 F4/80 consistent with macrophage identity. At 7d %EDU$^+$ was 75±2.2% (mean±SD, n=4), but
29 96% of cells were SAβG-positive; 100% macrophages were SAβG$^+$ at both 21d and 28d when
30 EdU$^+$ remained high at 26% and 27% respectively (**Supplementary Material** online, *Figure*
31 *S5*). IL6 expression did not increase over time (**Supplementary Material** online, *Figure S5*),
32 indicating that SAβG expression in macrophages does not correlate with a senescent pro-
33 inflammatory phenotype, but also occurs in proliferating macrophages. BMDMs had low p16
34 mRNA expression, but this increased >32-fold at 7d, and increased further at 21d and 28d**.**
35 p16 protein expression followed similar pattern to mRNA, and similar to of higher expression
36 than VSMCs undergoing SIPS (**Supplementary Material** online, **Figure S6)**. This data
37 indicates that differentiated mouse BMDMs show high SAβG activity and markedly increased
38 p16 expression, even in cells that maintain proliferation and do not express other SASP
39 markers such as IL6. In addition, p16 expression in differentiated mouse macrophages is
40 similar to or higher than expression of mouse VSMCs undergoing SIPS.
41
42 **3.5. Mouse VSMCs express p16 in atherosclerosis**
43 p16-expressing cells in human atherosclerotic plaque have been proposed to be of VSMC
44 origin[2]. However, as VSMCs lose lineage markers when they de-differentiate and can gain
45 'macrophage markers'[21] and macrophages express p16 (**Supplementary Material** online,
46 *Figure S6*), the lineage of p16$^+$ cells in plaques is unclear. Indeed, we found that human
47 plaques contain p16$^+$ cells that express conventional VSMC markers such as αSMA or
48 macrophage markers such as CD68 (**Supplementary Material** online, *Figure S7*). In
49 contrast, VSMCs and their progeny can be identified in mouse atherosclerosis by Cre-Lox
50 mediated induction of reporter expression specifically in smooth muscle cells, for example in
51 Myh11-Cre^{ERt2}/Rosa26-Confetti mice; flow cytometric sorting of isolated confetti$^+$ cells
52 followed by single cell sequencing (scRNA-seq) can then quantify mRNA expression
53 specifically in VSMCs[14,22]. Normal healthy aortas of Myh11-Cre^{ERt2}/ Rosa26-Confetti mice
54 showed cell clusters corresponding to VSMCs (Myh11$^+$), adventitial cells (Pdgfra$^+$) or

1   endothelial cells (Cdh5^{+})(***Figure 2A***). p16 (Cdkn2a) showed very low expression in all cell
2   clusters **(*Figure 2A*),** suggesting few senescent cells in normal vessels. In contrast,
3   p16[+]/Cdkn2a was detected in confetti[+] VSMC-derived cells from atherosclerotic plaques of fat-
4   fed of Myh11-Cre[ERt2]/Rosa26-Confetti/ApoE^{-/-} animals (***Figure 2B***). Interestingly, p16[+] VSMCs
5   were predominantly located in VSMCs with lower expression of Myh11 (Clusters 6,8,9), CD68
6   (Cluster 11), or VSMCs expressing the stem cell marker Sca-1/Ly6a, which is a VSMC
7   phenotype that is associated with cell activation[14] **(*Figure 2B, C*)**.
8
9   **3.6. Effects of ablation of p16^{+} cells in atherosclerosis**
10 Recent studies suggest that senescent cells in multiple tissues (including mouse
11 atherosclerotic plaques) can be removed by p16-promoter-driven suicide genes[5,19,23,24], and
12 we find that GCV selectively kills senescent p16-3MR mouse VSMCs *in vitro* **(Supplementary**
13 **Material** online, **Figure S4)**. We therefore crossed C57BL/6J p16-3MR with C57BL/6J ApoE[-
14 /-] mice and studied atherosclerosis after chronic ablation of p16-expressing cells. To examine
15 the effect of selective removal of p16^{+} cells in either the vessel wall or bone marrow-derived
16 cells, we irradiated and transplanted ApoE^{-/-} mice either with p16-3MR/ApoE^{-/-} (p16→ApoE)
17 or ApoE^{-/-} marrow (ApoE→ApoE), or p16-3MR/ApoE^{-/-} mice with either p16-3MR/ApoE^{-/-}
18 (p16→p16) or ApoE^{-/-} bone marrow (ApoE→p16). Bone marrow reconstitution was near 100%
19 for p16-3MR or ApoE^{-/-} transplants **(Supplementary Material** online, ***Figure S8A***), and
20 showed similar blood counts in all groups prior to administration of GCV or saline. p16→p16
21 mice were further divided into two groups, one receiving GCV and one receiving saline control.
22 Thus, we have two control groups (ApoE→ApoE and p16→p16 mice that received saline),
23 and three experimental groups for removal of either all p16^{+} cells (p16→p16 +GCV), or to
24 selectively ablate bone marrow-derived (p16→ApoE +GCV), or vessel wall-derived p16^{+} cells
25 (ApoE→p16 +GCV).
26
27 As demonstrated previously[19], the p16-3MR transgene is activated by irradiation in mice,
28 manifesting as luciferase activity by bioluminescence after substrate injection
29 **(Supplementary Material** online, ***Figure S8B***), confirming that irradiation does not prevent
30 cells becoming senescent. Male and female mice were fat fed from 8-22w of age, and treated
31 with 3 cycles of 5mg/kg/day GCV or saline control for 5 days starting at 12w of age, followed
32 by 2w recovery, a dosing regimen shown to efficiently ablate p16^{+} cells in p16-3MR mice in
33 other studies[5,19]. Body weight, blood pressure, blood counts, serum lipids, and a range of
34 serum inflammatory cytokines were similar in all groups **(Supplementary Material** online,
35 ***Supplemental Table 1***). At 22w vascular beds were examined for plaque size and
36 composition (aortic root: fibrous cap and necrotic core size) and % plaque area (descending
37 aorta), There was no difference in aortic root plaque size between the controls (ApoE→ApoE
38 + saline and p16→p16 mice + saline). Interestingly, we also found no detectable difference in
39 plaque size, or cap or core sizes relative to plaque area or each other in any experimental vs.
40 any control group **(*Figure 3A-B,* Supplementary Material** online, ***Figure S8C-E***). Percentage
41 plaque area in the descending aorta was also similar in all groups **(Supplementary Material**
42 online, ***Figure S8F*).**
43
44 GCV induces apoptosis in cells expressing HSV TK[25] and this mechanism underlies its ability
45 to clear p16-3MR reporter gene-expressing cells. However, atherosclerosis is associated with
46 defective efferocytosis[26], and both VSMC and macrophage apoptosis in atherosclerosis can
47 be associated with inflammation, which can promote atherogenesis[27,28]. The number of
48 TUNEL^{+} apoptotic cells in aortic root plaques was increased in GCV-treated p16→p16 mice
49 (which express p16-3MR in both vessel wall and bone marrow-derived cells), and in GCV-
50 treated p16→ApoE mice (which express p16-3MR in vessel wall-derived cells), with similar
51 appearances of the TUNEL[+] cellular debris in the plaque cores (***Figure 3A,C***). GCV-treated
52 p16→p16 mice also showed increased Mac3^{+} cells as a marker of macrophage content (vs.
53 both controls and GCV-treated ApoE→p16 mice), and increased expression of p16 (vs. GCV-
54 treated ApoE→ApoE mice), IL18 (vs. saline-treated p16→p16 mice), TNFα (vs. both controls

1   and GCV-treated ApoE→p16 mice (*Figure 3D-G*), and Mac3 (vs. saline-treated p16→p16
2   mice)(**Supplementary Material** online, *Figure S9*). suggesting an influx of p16$^+$ macrophages
3   in GCV-treated p16→p16 mice.
4
5   This data strongly suggests that cyclical GCV-induced killing of p16$^+$ cells within plaques
6   induces inflammation, most likely due to defective efferocytosis of p16$^+$ cells due to reduced
7   tissue macrophages that clear senescent cells, and an influx of circulating p16$^+$
8   monocyte/macrophages in GCV-treated p16→p16 mice. The precise macrophage subtype
9   responsible for senescent cell clearance in atherosclerosis is unclear, but tissue macrophages
10 expressing the leukocyte integrin CD11d$^+$ clear senescent cells in the spleen[29]. CD11d
11 expression was increased in GCV-treated ApoE→p16 mice (which express p16-3MR in vessel
12 wall-derived cells) against all the other groups, while expression of CD11b and the M1 and
13 M2 macrophage markers NOS2 and ARG1 respectively were similar in all mice
14 (**Supplementary Material** online, *Figure S9*).
15
16 **3.7. The senolytic ABT-263 (navitoclax) selectively kills senescent mouse VSMCs**
17 Senolytics are a new class of drugs that selectively induce apoptosis in senescent cells, often
18 by targeting senescent cell anti-apoptotic pathways (SCAPs) such as BCL2 and BCL$_{XL}$ family
19 proteins, the PI3K-AKT axis, and HSP90 (reviewed in [30]). Interestingly, while some senolytics
20 such as ABT-263 can remove senescent cells in tissues[17,31], including in atherosclerotic
21 plaques[5], other agents, such as quercetin and dasatinib had no effect on plaque development
22 or composition[12]. We therefore examined the ability of ABT-263, the most widely studied
23 senolytic, to selectively induce apoptosis in senescent mouse VSMCs *in vitro*, prior to
24 assessing its effect on atherogenesis.
25
26 1μM ABT-263 had no significant effect on cell number in replicating mouse VSMCs, or cell
27 proliferation (%EdU$^+$) in either replicating VSMCs or those treated with Dox 1+ 7d, although
28 higher doses induced cell death (**Supplementary Material** online, *Figure S10*). Dox 1+ 7d
29 treatment of replicating mouse VSMCs induced cell senescence with increased %SAβG$^+$ cells;
30 ABT-263 significantly reduced %SAβG$^+$ cells in senescent but not replicating VSMCs (*Figure
31 4A-B*). ABT-263 also reduced expression of p16 protein and mRNA of p16 and the SASP
32 cytokines IL18 and TNFα, but not IL6 (*Figure 4C-D*), all together suggesting that ABT-263
33 selectively kills senescent *vs.* proliferating VSMCs. However, macrophage survival is
34 dependent upon expression of BCL2 family members, such that BCL2 knockout promotes
35 macrophage apoptosis and necrotic core formation in plaques in mice[32]. ABT-263 also
36 induced cell death of cultured bone marrow-derived macrophages above 1μM
37 (**Supplementary Material** online, *Figure S11*), and this did not depend upon expression of
38 SAβG (*Figure 4E*).
39
40 **3.8. ABT-263 reduces atherosclerosis**
41 To determine whether ABT-263 could reduce atherogenesis, we fat fed male and female
42 ApoE$^{-/-}$ mice from 8-22w, and administered 3 cycles of vehicle control or 50mg/kg/day ABT-
43 263 by daily oral gavage for 5 days followed by 3w recovery, a regimen previously
44 demonstrated to efficiently remove senescent cells in mice[16,17]. There was no difference in
45 body weight, mean blood pressure, or serum lipids between control and ABT-263-treated mice
46 (**Supplementary Material** online, *Table S2*). However, ABT-263 treatment reduced
47 atherosclerosis lesion area in both the descending aorta and aortic root, with a reduction in
48 absolute core but not cap area (*Figure 5A-E*), but not relative cap or core areas
49 (**Supplementary Material** online, *Figure S12*). ABT-263 treatment did reduce %mac3+ cells
50 in plaques by immunohistochemistry but not mac3 mRNA expression (**Supplementary
51 Material** online, *Figure S13*).
52
53 To examine whether ABT-263 inhibited atherosclerosis through senolysis, we examined both
54 SASP cytokine levels in serum or mRNAs in the aorta of control and ABT-263-treated mice.

1 Serum IL-6 was markedly reduced by ABT-263 treatment (45.36pg/ml (21.5) vs. 138.8pg/ml
2 (116.3), mean (SD), p=0.0068), but other serum cytokines were unchanged **(Supplementary**
3 **Material** online, *Table S2*)**. Similarly, despite limitations in their use as senescence markers
4 in atherosclerosis, there was no effect of ABT-263 treatment on expression of p16 or a range
5 of SASP cytokine mRNAs in the vessel wall **(*Figure 5F*)**, raising the possibility that some of
6 the effects of ABT-263 may not be through senolysis.
7
8 ABT-263 induces dose-limiting thrombocytopenia due to platelets requiring BCL_{XL} for survival,
9 and $BCL2/BCL_{XL}$ also regulate monocyte/macrophage and neutrophil survival[33,34]; we
10 therefore examined the effect of cycles of ABT-263 on blood counts. ABT-263 significantly
11 reduced total leukocyte count, platelet count and lymphocyte counts between baseline and
12 sacrifice (**Figure 6A-F**), suggesting that some of the anti-atherogenic effects of ABT-263 may
13 be due to reductions in leukocytes and platelets rather than entirely through senolysis.
14
15

1 **4. Discussion**
2
3 Cell senescence has been identified in most if not all organs in humans. Clearance of
4 senescent cells or 'Senolysis' can increase health span and ameliorate a wide range of aging-
5 associated diseases[5,19,23,24], such that senolytic pharmacotherapy has been heralded as a new
6 therapeutic modality, including in atherosclerosis. However, senescence markers (and thus
7 targets) vary with species, inducer and cell type. Furthermore, senolysis relies upon sensitive
8 and specific markers for senescent cells that are not expressed in non-senescent resident
9 cells, and agents with no deleterious consequences or side effects. Our study indicates that
10 senolysis using p16-coupled therapies and ABT-263 are not specific and may lead to other
11 processes that limit their effectiveness.
12
13 We examined the sensitivity and specificity of p16, a transgenic p16 reporter-construct (p16-
14 3MR), Lamin B1 and SAβG to identify senescent VSMCs, and the effects of both genetic and
15 pharmacological senolysis. The study presents a number of novel and important findings,
16 namely: **(a)** p16 expression is increased and Lamin B1 expression is decreased in cultured
17 human VSMCs undergoing senescence, but the kinetics of appearance/disappearance of p16
18 and Lamin B1 are different, **(b)** increased p16 and SAβG activity and reduced Lamin B1 occur
19 in both RS and SIPS of cultured human VSMCs, but, similar to other studies[35], p16 mRNA
20 expression increases <4-fold, **(c)** Similarly, p16 and SAβG activity increases and Lamin B1
21 expression decreases in mouse VSMCs undergoing SIPS, but p16 mRNA increases <2-fold,
22 **(d)** in contrast, p16 and SAβG activity increase markedly during differentiation of cultured
23 macrophages, and are expressed by proliferating macrophages. Thus, p16 and SAβG are not
24 markers of senescence in macrophages, and the >32-fold increase in p16 in differentiating
25 macrophages compared with the <4-fold increase in senescent human and mouse VSMCs
26 suggests that identification or removal of senescent cells using p16 has a small selective
27 window in atherosclerosis, **(e)** p16$^+$ VSMCs are detected in mouse atherosclerotic plaques
28 using scRNAseq; although these may be senescent VSMCs, they are also seen in clusters
29 that express macrophage markers or Ly6a/Sca1, (**f**) GCV treatment of fat-fed ApoE$^{-/-}$ mice
30 expressing p16-3MR globally or selectively in the vessel wall or bone marrow-derived cells
31 increases apoptotic cells and induces inflammation when expressed in both compartments,
32 but does not affect atherosclerosis extent or composition, **(g)** ABT-263 selectively kills
33 senescent vs. replicating mouse VSMCs, but can also kill macrophages, **(h)** ABT-263 reduces
34 atherosclerosis extent and absolute core size, **(i)** ABT-263 reduces serum IL6 levels, but does
35 not reduce vessel wall p16 or multiple SASP markers, **(j)** ABT-263 significantly reduces
36 leukocyte, monocyte, lymphocyte and platelet counts.
37
38 We find that the combination of loss of cell proliferation and LaminB1 expression and
39 increased p16 and SAβG are robust markers of human VSMC senescence *in vitro*. Mouse
40 VSMCs also increase SAβG on SIPS, but p16 upregulation is minimal, which may limit its
41 sensitivity to mark and remove senescence VSMCs in atherosclerosis models. p16 is also
42 expressed in resident and inflammatory macrophages, including macrophage-rich lesions in
43 human atherosclerotic plaques (seen here and [36]), and is upregulated when monocytes
44 differentiate into macrophages[37], for example in atherosclerosis. p16 can also regulate
45 macrophage polarisation, and promote inflammatory signaling in murine macrophages[38], and
46 phagocytic cells have SAβG activity in chronologically aged mice suggesting that they are
47 macrophages. Furthermore, macrophage removal reduces the p16^{ink4a} signal in p16^{ink4a}
48 reporter mice[39], and expression of p16 and SAβG are reversible in macrophages[9], suggesting
49 that p16 is another checkpoint in macrophage polarisation, and that these markers do not
50 necessarily indicate senescence[40]. These studies and our findings suggest significant
51 limitations in using p16, p16 reporters, or p16-linked suicide genes and SAβG to identify and/or
52 remove senescent cells in atherosclerosis.
53

1 We found no effect on atherosclerosis size or composition following GCV treatment of p16-
2 3MR/ApoE$^{-/-}$ mice. This contrasts with a study where GCV treatment of Ldlr$^{-/-}$/p16-3MR mice
3 reduced SAβG$^+$ cells, atherosclerosis extent, expression of inflammatory cytokines (IL1α,
4 TNFα, MCP-1, MMPs 3, 12 and 13), and p16[5]. This study concluded that GCV reduced
5 atherosclerosis by removing senescent cells[5], although detection and removal of SAβG$^+$ cells
6 in fatty streaks within 9 days of fat feeding suggests these cells may represent newly migrated
7 macrophages, not senescent cells. However, there are also significant methodological
8 differences between the studies that could explain the different observations. We used ApoE$^-$
9 $^{/-}$ mice, which have much larger and more advanced lesions than Ldlr$^{-/-}$ mice on fat feeding,
10 and different time points and diets for the mice. Our mice also underwent irradiation, which
11 induces senescent cells that are evident 3 months later[41], and can be removed by GCV in
12 p16-3MR mice[41], indicating that the response to GCV and p16-3MR activation is not different
13 before and after irradiation. Irradiation has variable effects on lesion size, with no change in
14 brachiocephalic plaques[42], increased lesions in aortic roots or reduced lesions in descending
15 aorta[43]. However, all our mice underwent comparable irradiation and reconstitution with
16 syngeneic bone marrow, yet we saw significantly different effects on cell death and
17 inflammation induced by GCV between groups, and irradiation activated the p16-3MR
18 transgene. Any lack of difference in plaque size between groups is therefore not due to
19 inadequate transgene activation or GCV dose, vessel wall cell adaptation to the earlier stress
20 generated by irradiation, or that irradiation and bone marrow transplant significantly reduce
21 development of senescent VSMCs during atherosclerosis.
22
23 It has been suggested that off-target effects of senolytics could be reduced by a 'hit-and-run'
24 strategy. However, we find that cyclically inducing apoptosis of senescent cells can result in a
25 number of potentially detrimental effects, including inflammation and bone marrow
26 suppression (**Figure 6G,H**). For example, we observe increased inflammation in GCV-treated
27 p16$\rightarrow$p16 mice, which may represent increased migration of p16$^+$ macrophages, consistent
28 with studies showing that senescent cells preferentially attract macrophages characterised by
29 p16^{Ink4a} gene expression and β-galactosidase activity[39]. Inflammation may negate any positive
30 effect of deleting senescent cells, while increased CD11d$^+$ cells in ApoE$\rightarrow$p16 mice may clear
31 senescent VSMCs and dampen any inflammation induced by their killing. CD11d/CD18 is
32 expressed at a basal level on the surface of all leukocytes, but is up-regulated on phagocytic
33 leukocytes present in regions of local inflammation, and CD11d$^+$ macrophages clear
34 senescent erythrocytes in the spleen[29]. Our data is therefore consistent with studies that show
35 that deleting p16$^+$ cells can have neutral or detrimental effects in development, wound healing
36 and a variety of disease states[10,11,19,44,45]. While cycles of ABT-263 do reduce atherosclerosis,
37 ABT-263 had no effect on tissue markers of cell senescence, and also results in a persistent
38 reduction in leukocytes and platelets. Thus, the efficacy of ABT-263 compared with p16-3MR-
39 based senolysis may be due to both systemic and local anti-inflammatory effects, only some
40 of which may be due to any senolytic action (**Figure 6H**).
41
42 Our study also identifies limitations on interpreting studies on senescence. First, it is not
43 possible currently to provide an absolute frequency of VSMC senescence in atherosclerosis.
44 Cell senescence is not a static cellular state, but a multistep process where cells undergo pre-
45 senescence/quiescence, stable growth arrest, full senescence (chromatin changes
46 associated with SASP) and late/deep senescence (phenotypic change/diversification)[46]. The
47 stage at which VSMCs express particular senescence markers in tissues is not known, and,
48 as demonstrated here, we lack sensitive and specific markers of VSMC senescence in
49 atherosclerosis. VSMCs (and other cells) also lose their lineage markers in disease, such that
50 the identity of αSMA-negative cells expressing senescence markers is unknown unless
51 genetic lineage marking is employed. While the scRNAseq of Myh11-cre^{ERT2}/Rosa26-Confetti$^+$
52 system provides lineage markers, lowly expressed genes may not be detected by scRNA-seq.
53 Furthermore, senescent cells are often larger than replicating cells and may be selectively
54 depleted by flow sorting of cells prior to scRNA-seq analysis.

1
2 Rather, we can conclude that certain conditions, for example atherosclerosis, and regions
3 within the plaque (e.g. fibrous cap), show higher frequencies of cells expressing markers
4 associated with senescence than undiseased vessels. VSMC senescence promotes
5 atherosclerosis[6,7] and prevention of VSMC senescence delays atherogenesis[6]; however,
6 whether senolytic drugs as a group reduce atherosclerosis, and whether any effect is entirely
7 through removal of senescent cells is still unclear. While the anti-atherogenic effects of ABT-
8 263 are encouraging, macrophage deficiency of BCL2 increases their apoptosis in
9 atherosclerosis[32], and monocyte/macrophage apoptosis reduces plaque development[27], such
10 that agents that target BCL2/BCL$_{XL}$ such as ABT-263 might act by removing macrophages or
11 other leukocytes, and not just through removing senescent cells.
12
13 In summary, we identify significant limitations of p16 and p16-driven reporter genes to both
14 identify and remove senescent cells in atherosclerosis, and adverse local or systemic
15 consequences of p16 or ABT-263-mediated senolysis. Our study suggests that conclusions
16 from previous studies of atherosclerosis utilising p16 or ABT-263 should be reassessed, while
17 preclinical testing of current and novel senolytics requires the development of sensitive and
18 lineage-specific markers of cell senescence in atherosclerosis before ascribing effects entirely
19 to senolysis.
20

References

1. Wang JC, Bennett M. Aging and atherosclerosis: mechanisms, functional consequences, and potential therapeutics for cellular senescence. *Circ Res*. 2012;**111**:245-259.

2. Matthews C, Gorenne I, Scott S, Figg N, Kirkpatrick P, Ritchie A, Goddard M, Bennett M. Vascular smooth muscle cells undergo telomere-based senescence in human atherosclerosis: effects of telomerase and oxidative stress. *Circ Res*. 2006;**99**:156-164.

3. Gardner SE, Humphry M, Bennett MR, Clarke MC. Senescent vascular smooth muscle cells drive inflammation through an Interleukin-1alpha-dependent senescence-sssociated secretory phenotype. *Arterioscler Thromb Vasc Biol*. 2015;**35**:1963-1974.

4. Calvert P, Liew T, Gorenne I, Clarke M, Costopoulos C, Obaid D, O'Sullivan M, Shapiro L, McNab D, Densem C, Schofield P, Braganza D, Clarke S, Ray K, West N, Bennett M. Leukocyte telomere length is associated with high-risk plaques on virtual histology intravascular ultrasound and increased pro-inflammatory activity. *ATVB*. 2011;**31**:2157-2164.

5. Childs BG, Baker DJ, Wijshake T, Conover CA, Campisi J, van Deursen JM. Senescent intimal foam cells are deleterious at all stages of atherosclerosis. *Science*. 2016;**354**:472-477.

6. Wang J, Uryga AK, Reinhold J, Figg N, Baker L, Finigan A, Gray K, Kumar S, Clarke M, Bennett M. Vascular smooth muscle cell senescence promotes atherosclerosis and features of plaque vulnerability. *Circulation*. 2015;**32**:1909-1919.

7. Hamczyk MR, Villa-Bellosta R, Gonzalo P, Andres-Manzano MJ, Nogales P, Bentzon JF, Lopez-Otin C, Andres V. Vascular Smooth Muscle-Specific Progerin Expression Accelerates Atherosclerosis and Death in a Mouse Model of Hutchinson-Gilford Progeria Syndrome. *Circulation*. 2018;**138**:266-282.

8. Frescas D, Hall BM, Strom E, Virtuoso LP, Gupta M, Gleiberman AS, Rydkina E, Balan V, Vujcic S, Chernova OB, Gudkov AV. Murine mesenchymal cells that express elevated levels of the CDK inhibitor p16(Ink4a) in vivo are not necessarily senescent. *Cell Cycle*. 2017;**16**:1526-1533.

9. Hall BM, Balan V, Gleiberman AS, Strom E, Krasnov P, Virtuoso LP, Rydkina E, Vujcic S, Balan K, Gitlin, II, Leonova KI, Consiglio CR, Gollnick SO, Chernova OB, Gudkov AV. p16(Ink4a) and senescence-associated beta-galactosidase can be induced in macrophages as part of a reversible response to physiological stimuli. *Aging (Albany NY)*. 2017;**9**:1867-1884.

10. de Mochel NR, Cheong KN, Cassandras M, Wang C, Krasilnikov M, Matatia P, Molofsky A, Campisi J, Peng T. Sentinel p16INK4a+ cells in the basement membrane form a reparative niche in the lung. *bioRxiv*. *https://doi.org/10.1101/2020.06.10.142893*. 2020.

11. Grosse L, Wagner N, Emelyanov A, Molina C, Lacas-Gervais S, Wagner KD, Bulavin DV. Defined p16(High) Senescent Cell Types Are Indispensable for Mouse Healthspan. *Cell Metab*. 2020;**32**:87-99 e86.

12. Roos CM, Zhang B, Palmer AK, Ogrodnik MB, Pirtskhalava T, Thalji NM, Hagler M, Jurk D, Smith LA, Casaclang-Verzosa G, Zhu Y, Schafer MJ, Tchkonia T, Kirkland JL, Miller JD. Chronic senolytic treatment alleviates established vasomotor dysfunction in aged or atherosclerotic mice. *Aging Cell*. 2016;**15**:973-977.

13. Tabas I. Consequences and therapeutic implications of macrophage apoptosis in atherosclerosis: the importance of lesion stage and phagocytic efficiency. *Arterioscler Thromb Vasc Biol*. 2005;**25**:2255-2264.

14. Dobnikar L, Taylor AL, Chappell J, Oldach P, Harman JL, Oerton E, Dzierzak E, Bennett MR, Spivakov M, Jorgensen HF. Disease-relevant transcriptional signatures identified in individual smooth muscle cells from healthy mouse vessels. *Nat Commun*. 2018;**9**:4567.

15. Yu E, Calvert PA, Mercer JR, Harrison J, Baker L, Figg NL, Kumar S, Wang JC, Hurst LA, Obaid DR, Logan A, West NE, Clarke MC, Vidal-Puig A, Murphy MP, Bennett MR. Mitochondrial DNA damage can promote atherosclerosis independently of reactive oxygen species through effects on smooth muscle cells and monocytes and correlates with higher-risk plaques in humans. *Circulation*. 2013;**128**:702-712.

16. Chang J, Wang Y, Shao L, Laberge RM, Demaria M, Campisi J, Janakiraman K, Sharpless NE, Ding S, Feng W, Luo Y, Wang X, Aykin-Burns N, Krager K, Ponnappan U, Hauer-Jensen M, Meng A, Zhou D. Clearance of senescent cells by ABT263 rejuvenates aged hematopoietic stem cells in mice. *Nat Med*. 2016;**22**:78-83.

17. Pan J, Li D, Xu Y, Zhang J, Wang Y, Chen M, Lin S, Huang L, Chung EJ, Citrin DE, Wang Y, Hauer-Jensen M, Zhou D, Meng A. Inhibition of Bcl-2/xl With ABT-263 Selectively Kills Senescent Type II Pneumocytes and Reverses Persistent Pulmonary Fibrosis Induced by Ionizing Radiation in Mice. *Int J Radiat Oncol Biol Phys*. 2017;**99**:353-361.

18. Noureddine H, Gary-Bobo G, Alifano M, Marcos E, Saker M, Vienney N, Amsellem V, Maitre B, Chaouat A, Chouaid C, Dubois-Rande JL, Damotte D, Adnot S. Pulmonary artery smooth muscle cell senescence is a pathogenic mechanism for pulmonary hypertension in chronic lung disease. *Circ Res*. 2011;**109**:543-553.

19. Demaria M, Ohtani N, Youssef SA, Rodier F, Toussaint W, Mitchell JR, Laberge RM, Vijg J, Van Steeg H, Dolle ME, Hoeijmakers JH, de Bruin A, Hara E, Campisi J. An Essential Role for Senescent Cells in Optimal Wound Healing through Secretion of PDGF-AA. *Dev Cell*. 2014;**31**:722-733.

20. Robbins CS, Hilgendorf I, Weber GF, Theurl I, Iwamoto Y, Figueiredo JL, Gorbatov R, Sukhova GK, Gerhardt LM, Smyth D, Zavitz CC, Shikatani EA, Parsons M, van Rooijen N, Lin HY, Husain M, Libby P, Nahrendorf M, Weissleder R, Swirski FK. Local proliferation dominates lesional macrophage accumulation in atherosclerosis. *Nat Med*. 2013;**19**:1166-1172.

21. Shankman LS, Gomez D, Cherepanova OA, Salmon M, Alencar GF, Haskins RM, Swiatlowska P, Newman AA, Greene ES, Straub AC, Isakson B, Randolph GJ, Owens GK. KLF4-dependent phenotypic modulation of smooth muscle cells has a key role in atherosclerotic plaque pathogenesis. *Nat Med*. 2015;**21**:628-637.

22. Chappell J, Harman JL, Narasimhan VM, Yu H, Foote K, Simons BD, Bennett MR, Jorgensen HF. Extensive Proliferation of a Subset of Differentiated, yet Plastic, Medial Vascular Smooth Muscle Cells Contributes to Neointimal Formation in Mouse Injury and Atherosclerosis Models. *Circ Res*. 2016;**119**:1313-1323.

23. Baker DJ, Wijshake T, Tchkonia T, LeBrasseur NK, Childs BG, van de Sluis B, Kirkland JL, van Deursen JM. Clearance of p16Ink4a-positive senescent cells delays ageing-associated disorders. *Nature*. 2011;**479**:232-236.

24. Baker DJ, Childs BG, Durik M, Wijers ME, Sieben CJ, Zhong J, Saltness RA, Jeganathan KB, Verzosa GC, Pezeshki A, Khazaie K, Miller JD, van Deursen JM. Naturally occurring p16(Ink4a)-positive cells shorten healthy lifespan. *Nature*. 2016;**530**:184-189.

25. Laberge RM, Adler D, DeMaria M, Mechtouf N, Teachenor R, Cardin GB, Desprez PY, Campisi J, Rodier F. Mitochondrial DNA damage induces apoptosis in senescent cells. *Cell Death Dis*. 2013;**4**:e727.

26. Schrijvers DM, De Meyer GR, Kockx MM, Herman AG, Martinet W. Phagocytosis of apoptotic cells by macrophages is impaired in atherosclerosis. *Arterioscler Thromb Vasc Biol*. 2005;**25**:1256-1261.

27. Stoneman V, Braganza D, Figg N, Mercer J, Lang R, Goddard M, Bennett M. Monocyte/macrophage suppression in CD11b diphtheria toxin receptor transgenic mice differentially affects atherogenesis and established plaques. *Circ Res*. 2007;**100**:884-893.

28. Clarke MC, Figg N, Maguire JJ, Davenport AP, Goddard M, Littlewood TD, Bennett MR. Apoptosis of vascular smooth muscle cells induces features of plaque vulnerability in atherosclerosis. *Nat Med.* 2006;**12**:1075-1080.

29. Van der Vieren M, Le Trong H, Wood CL, Moore PF, St J, T, Staunton DE, Gallatin WM. A novel leukointegrin, α d β 2, binds preferentially to ICAM-3. *Immunity.* 1995;**3**:683–690.

30. Kirkland JL, Tchkonia T, Zhu Y, Niedernhofer LJ, Robbins PD. The Clinical Potential of Senolytic Drugs. *J Am Geriatr Soc.* 2017;**65**:2297-2301.

31. Zhu Y, Tchkonia T, Fuhrmann-Stroissnigg H, Dai HM, Ling YY, Stout MB, Pirtskhalava T, Giorgadze N, Johnson KO, Giles CB, Wren JD, Niedernhofer LJ, Robbins PD, Kirkland JL. Identification of a novel senolytic agent, navitoclax, targeting the Bcl-2 family of anti-apoptotic factors. *Aging Cell.* 2014;**15**:428-435.

32. Thorp E, Li Y, Bao L, Yao PM, Kuriakose G, Rong J, Fisher EA, Tabas I. Brief report: increased apoptosis in advanced atherosclerotic lesions of Apoe-/- mice lacking macrophage Bcl-2. *Arterioscler Thromb Vasc Biol.* 2009;**29**:169-172.

33. Gautier EL, Huby T, Witztum JL, Ouzilleau B, Miller ER, Saint-Charles F, Aucouturier P, Chapman MJ, Lesnik P. Macrophage apoptosis exerts divergent effects on atherogenesis as a function of lesion stage. *Circulation.* 2009;**119**:1795-1804.

34. Shearn AI, Deswaerte V, Gautier EL, Saint-Charles F, Pirault J, Bouchareychas L, Rucker EB, 3rd, Beliard S, Chapman J, Jessup W, Huby T, Lesnik P. Bcl-x inactivation in macrophages accelerates progression of advanced atherosclerotic lesions in Apoe(-/-) mice. *Arterioscler Thromb Vasc Biol.* 2012;**32**:1142-1149.

35. Stojanovic SD, Fuchs M, Kunz M, Xiao K, Just A, Pich A, Bauersachs J, Fiedler J, Sedding D, Thum T. Inflammatory Drivers of Cardiovascular Disease: Molecular Characterization of Senescent Coronary Vascular Smooth Muscle Cells. *Front Physiol.* 2020;**11**:520.

36. Holdt LM, Sass K, Gabel G, Bergert H, Thiery J, Teupser D. Expression of Chr9p21 genes CDKN2B (p15(INK4b)), CDKN2A (p16(INK4a), p14(ARF)) and MTAP in human atherosclerotic plaque. *Atherosclerosis.***214**:264-270.

37. Fuentes L, Wouters K, Hannou SA, Cudejko C, Rigamonti E, Mayi TH, Derudas B, Pattou F, Chinetti-Gbaguidi G, Staels B, Paumelle R. Downregulation of the tumour suppressor p16INK4A contributes to the polarisation of human macrophages toward an adipose tissue macrophage (ATM)-like phenotype. *Diabetologia.***54**:3150-3156.

38. Cudejko C, Wouters K, Fuentes L, Hannou SA, Paquet C, Bantubungi K, Bouchaert E, Vanhoutte J, Fleury S, Remy P, Tailleux A, Chinetti-Gbaguidi G, Dombrowicz D, Staels B, Paumelle R. p16INK4a deficiency promotes IL-4-induced polarization and inhibits proinflammatory signaling in macrophages. *Blood.* 2011;**118**:2556-2566.

39. Hall BM, Balan V, Gleiberman AS, Strom E, Krasnov P, Virtuoso LP, Rydkina E, Vujcic S, Balan K, Gitlin I, Leonova K, Polinsky A, Chernova OB, Gudkov AV. Aging of mice is associated with p16(Ink4a)- and beta-galactosidase-positive macrophage accumulation that can be induced in young mice by senescent cells. *Aging (Albany NY).* 2016;**8**:1294-1315.

40. Behmoaras J, Gil J. Similarities and interplay between senescent cells and macrophages. *J Cell Biol.* 2021;**220**

41. Le ON, Rodier F, Fontaine F, Coppe JP, Campisi J, DeGregori J, Laverdiere C, Kokta V, Haddad E, Beausejour CM. Ionizing radiation-induced long-term expression of senescence markers in mice is independent of p53 and immune status. *Aging Cell.* 2010;**9**:398-409.

42. Newman AA, Baylis RA, Hess DL, Griffith SD, Shankman LS, Cherepanova OA, Owens GK. Irradiation abolishes smooth muscle investment into vascular lesions in specific vascular beds. *JCI Insight.* 2018;**3**

43. Schiller NK, Kubo N, Boisvert WA, Curtiss LK. Effect of gamma-irradiation and bone marrow transplantation on atherosclerosis in LDL receptor-deficient mice. *Arterioscler Thromb Vasc Biol.* 2001;**21**:1674-1680.

44. Munoz-Espin D, Canamero M, Maraver A, Gomez-Lopez G, Contreras J, Murillo-Cuesta S, Rodriguez-Baeza A, Varela-Nieto I, Ruberte J, Collado M, Serrano M. Programmed cell senescence during mammalian embryonic development. *Cell.* 2013;**155**:1104-1118.

45. Storer M, Mas A, Robert-Moreno A, Pecoraro M, Ortells MC, Di Giacomo V, Yosef R, Pilpel N, Krizhanovsky V, Sharpe J, Keyes WM. Senescence is a developmental mechanism that contributes to embryonic growth and patterning. *Cell.* 2013;**155**:1119-1130.

46. van Deursen J. The role of senescent cells in ageing. *Nature.* 2014;**509**:439-446.

1   **Figure Legends**
2
3   **Figure 1. Senescence markers in primary human and mouse VSMCs undergoing**
4   **senescence**
5   **(A)** % EdU$^+$ in cultured human VSMCs (Control), after 24h treatment with 500nM doxorubicin
6   (Dox 1d), after an additional 21 days recovery in control conditions (control 21d) or after
7   doxorubicin (Dox 1d+ 21d), or at replicative senescence (RS). **(B-D)** mRNA levels of Lamin
8   B1, p16 and p21 in cell populations described in **(A)** relative to control (1d) cells. **(E)** Western
9   blot for Lamin B1, p16, p21, and p53 for cells treated in **(A).** n=6-8 human VSMC isolates. **(F-**
10 **G)** EdU$^+$ % **(F)** or SAβG$^+$ % **(G)** of mouse p16-3MR VSMCs treated increasing concentrations
11 of Doxorubicin for 1d followed by 7d recovery vs. vehicle control. **(I-K)** qPCR for Lamin B1,
12 IL6, p16, or p21 mRNA expression for cells treated in **(F). (L)** Western blot of mouse cells as
13 treated in **(F)** for Lamin B1, p16, or p21. n=3-8 mouse VSMC isolates. Data are means (SD),
14 1-way ANOVA with correction for multiple comparisons **(A)** or unpaired Student t-test vs.
15 Control 1d **(B-D)** or vs. Vehicle (Dox 0nM)**(F-K).**
16
17 **Figure 2. p16/Cdkn2a is detected in VSMCs in mouse atherosclerotic plaques**
18 **(A-B)** UMAP plots showing scRNA-seq profiles of unsorted aortic cells from
19 Myh11Cre^{ERt2+}/Confetti$^+$ mice **(A)**, or sorted Confetti$^+$ VSMCs from atherosclerotic plaque and
20 media of fat-fed Myh11Cre^{ERt2}/Confetti$^+$/ApoE$^{-/-}$ mice **(B)**. Log-transformed expression levels
21 of Myh11 and p16/Cdkn2a are shown alongside e-Cadherin/Cdh5 and Pdgfrα **(A)** or Cd68
22 and Ly6a/Sca1 **(B)** using a scale from white to dark red. Insets show high power regions of
23 clusters 6, 8, and 9 and expression of p16 in **(B)**. Feature plots show log-normalized
24 expression levels. **(C)** % cells in each cluster with detectable expression of p16/cdkn2a after
25 14w or 18w or high fat feeding, or combined.
26
27 **Figure 3. GCV treatment of p16-3MR mice does not affect atherosclerosis, but induces**
28 **inflammation**
29 **(A)** Aortic root plaques in ApoE→ApoE, p16→ApoE, ApoE→p16, or p16→p16 mice + GCV,
30 or p16→p16 mice + saline, stained with Masson's trichrome, TUNEL, or Mac3. Scale
31 bar=300μm. High power inset shows apoptotic cell and nuclear debris from outlined area. **(B)**
32 Plaque area for mice in **(A). (C-D**) Number of TUNEL$^+$ cells/aortic root plaque **(C)** or %Mac3$^+$
33 cells **(D)** for mice in **(A). (E-G)** Relative mRNA expression for p16, IL18 or TNFα in
34 experimental mice. Data are means (SD) n=5-10 mice. 1-way ANOVA with correction for
35 multiple comparisons **(B-D)** or Kruskal-Wallis H Test followed by Dunn's multiple comparisons
36 test **(E-G).**
37
38 **Figure 4. ABT-263 (Navitoclax) selectively reduces senescent VSMCs**
39 **(A-B)** Photomicrographs **(A)** or quantification **(B)** of mouse VSMCs stained for SAβG, as
40 replicating control cells or after dox1+7d treatment, or each group ± 1μM ABT-263 treatment
41 for 48h**. (C)** Western blot and quantification for p16 in cells treated in **(A-B). (D)** Fold change
42 in mRNA expression compared with control replicating cells for p16 and a range of SASP
43 cytokines against the housekeeping gene HMBS. Data are means (SD), n=4-5. Unpaired
44 student t-test. **(E)** Mouse macrophages cultured for 28 days, then treated with 1μM ABT-263
45 for 48hrs and stained for SAβG. Data are means (SD), n=3. Unpaired student t-test.
46
47 **Figure 5. ABT-263 reduces atherosclerosis, but not local SASP cytokine expression**
48 **(A)** ORO staining of mouse descending aorta treated with control (vehicle) or ABT-263, and
49 quantification of %ORO area (n=11-14)**.** Scale bar=3mm. **(B)** Masson's trichrome
50 histochemistry of aortic root atherosclerotic plaque from mice treated in **(A).** Panels below
51 show high power view of outlined area. Arrow shows necrotic core. Scale bar=200μm. **(C-E)**
52 Aortic root Plaque area/Total area **(C)** Cap area **(D),** or Core area **(E)** for mice in **(A).** n=11-
53 13. **(F)** qPCR for relative expression of p16 or SASP cytokines in aortic arches of experimental

1 mice against the housekeeping gene HMBS (n=7). Data are means (SD), n=10. Unpaired
2 Student t-test **(A, C-E)** or Mann Whitney U test **(F).**
3
4 **Figure 6 Effects of ABT-263 on peripheral blood counts and overview of effects of**
5 **senolysis on atherosclerosis**
6 **(A-F)** Total red blood cell (RBC) and white blood cell (WBC) counts and differential WBC and
7 platelet counts in experimental mice at baseline and end of study after control treatment or
8 with ABT-263. Data are means (SD), n=12-15, Student t-test between baseline and end for
9 each group. **(G-H)** Schematic of predicted effects of GCV treatment on experimental mice and
10 observed or predicted consequences **(G),** or of ABT-263 on atherosclerosis and peripheral
11 blood counts **(H).**
12
13 **Graphical Abstract**
14 Effects of p16-induced genetic senolysis of ABT-263 drug-induced senolysis on
15 atherosclerosis.
16
17

Figure 1

Click here to access/download;Figure(s);Slide1.tiff

Figure 1

Figure 2

Figure 2

Figure 3

Figure 3

Figure 4
Click here to access/download;Figure(s);Slide4.tiff ⬇

Figure 4

Figure 5

Figure 5

Figure 6

Click here to access/download;Figure(s);Slide6.tiff ⬇
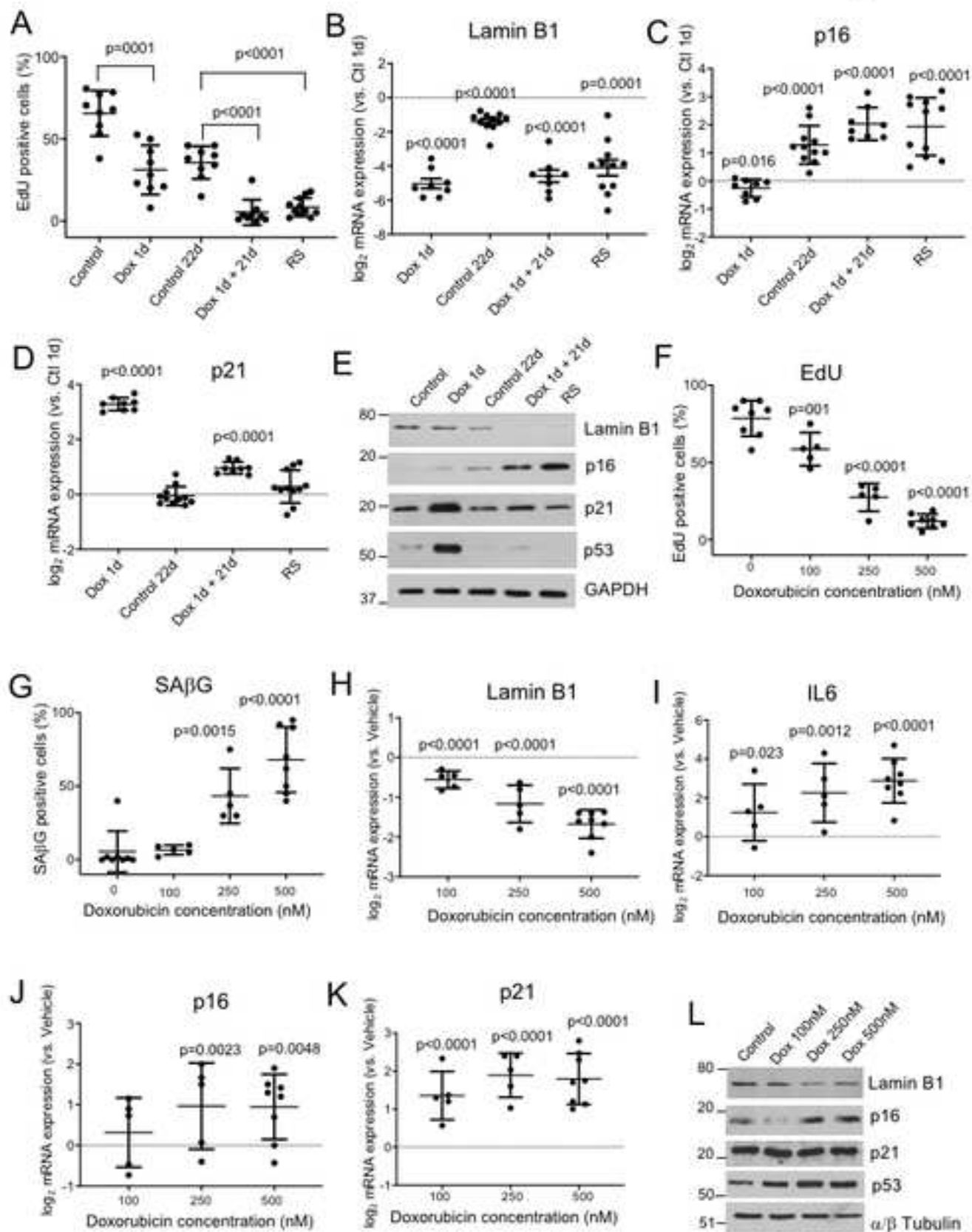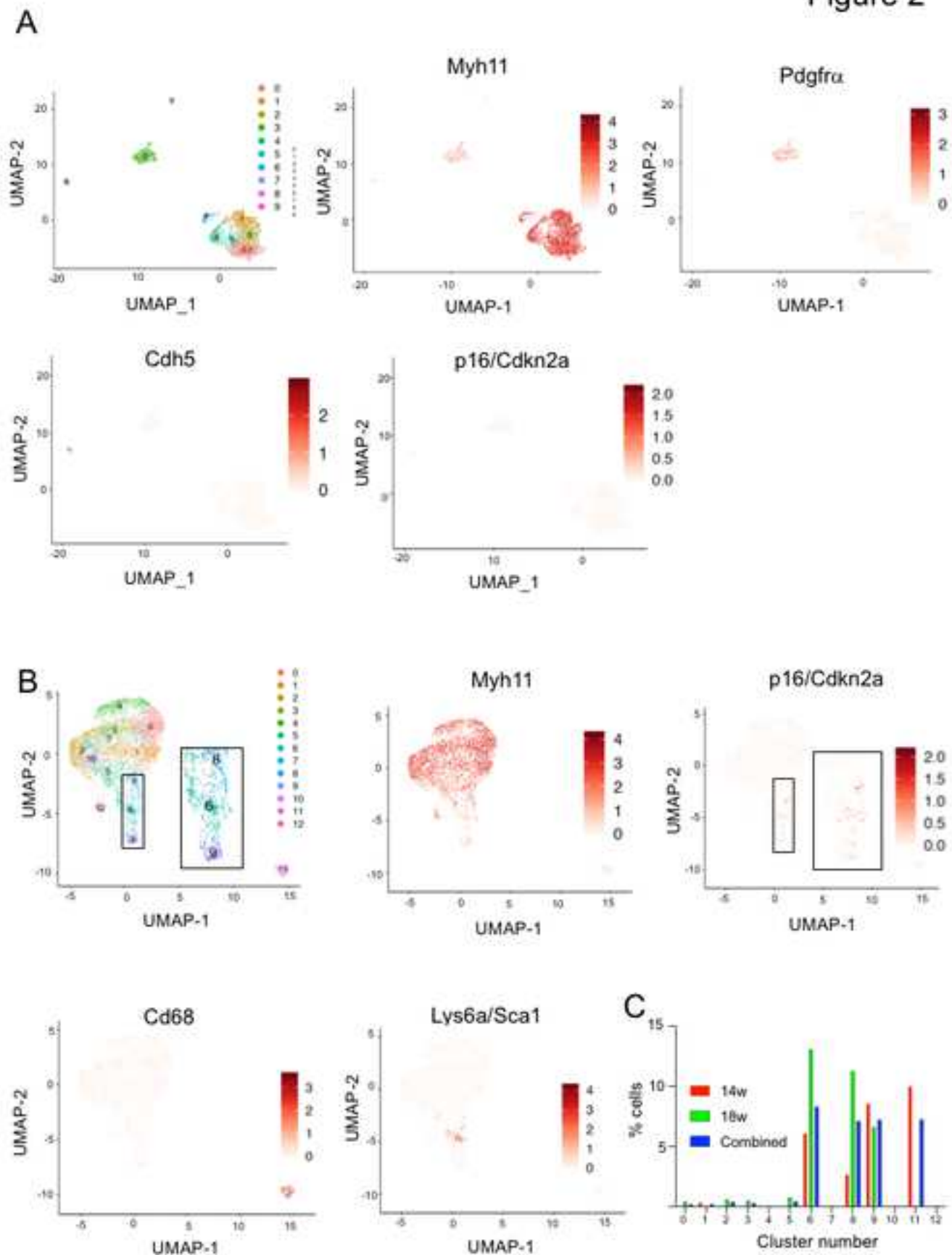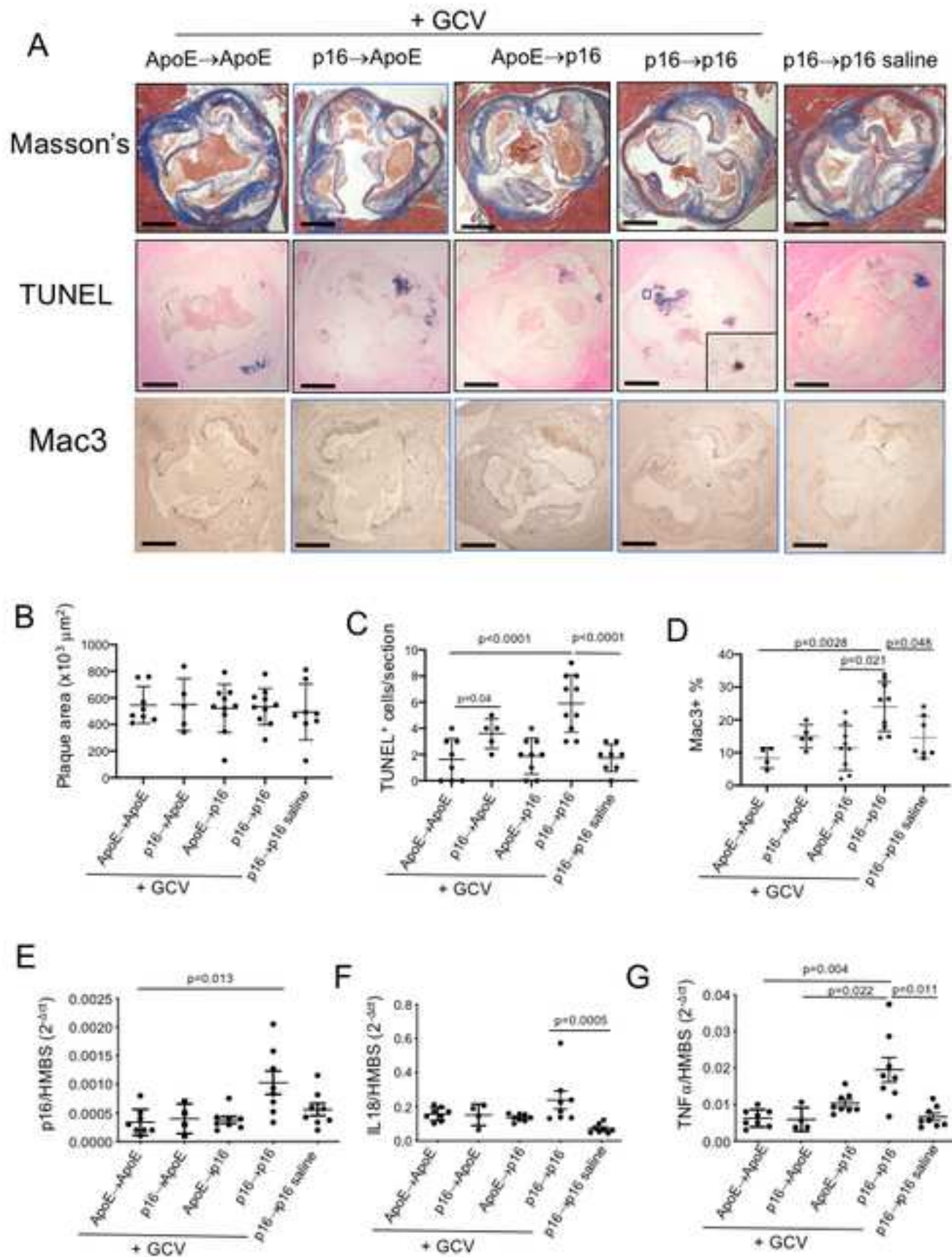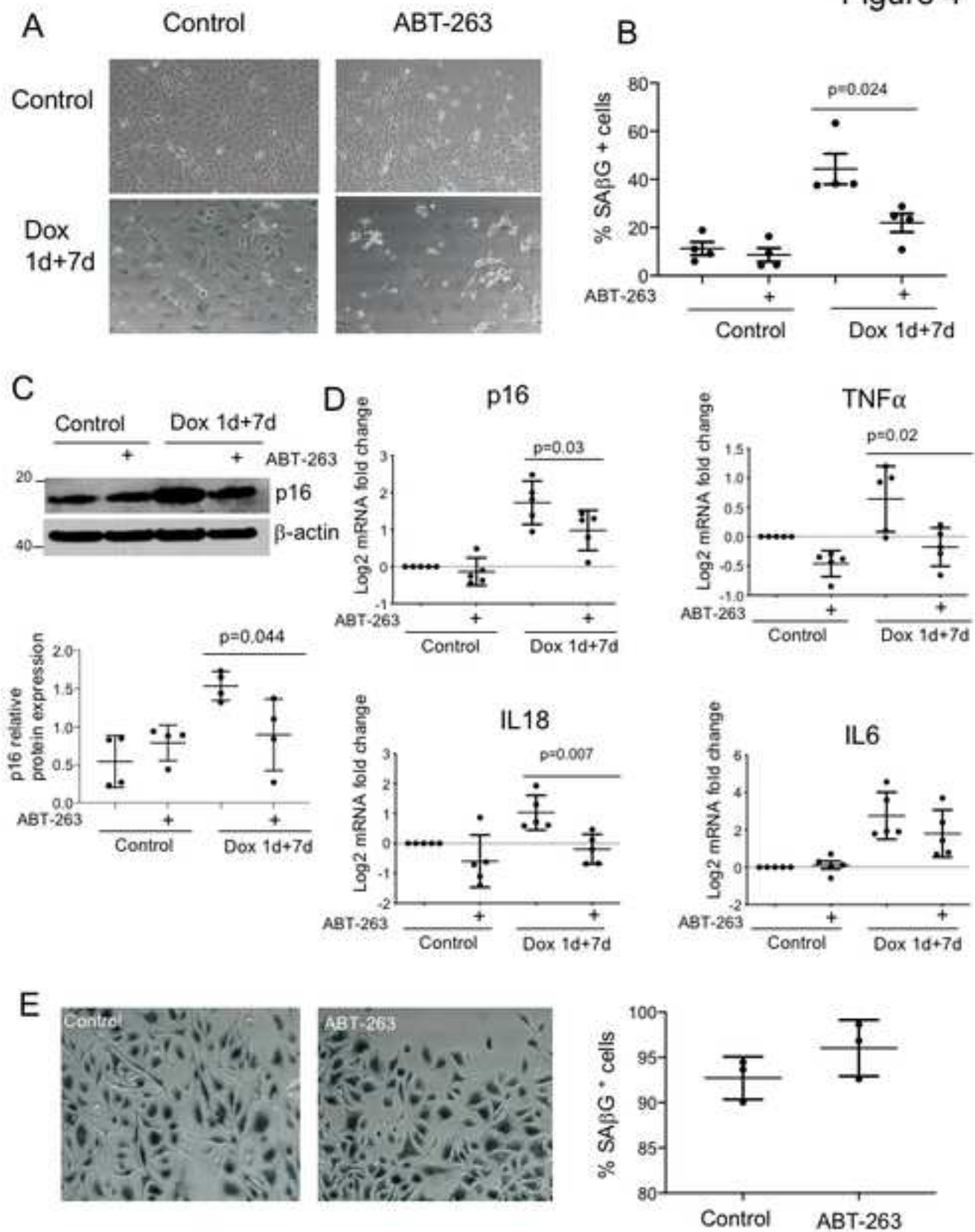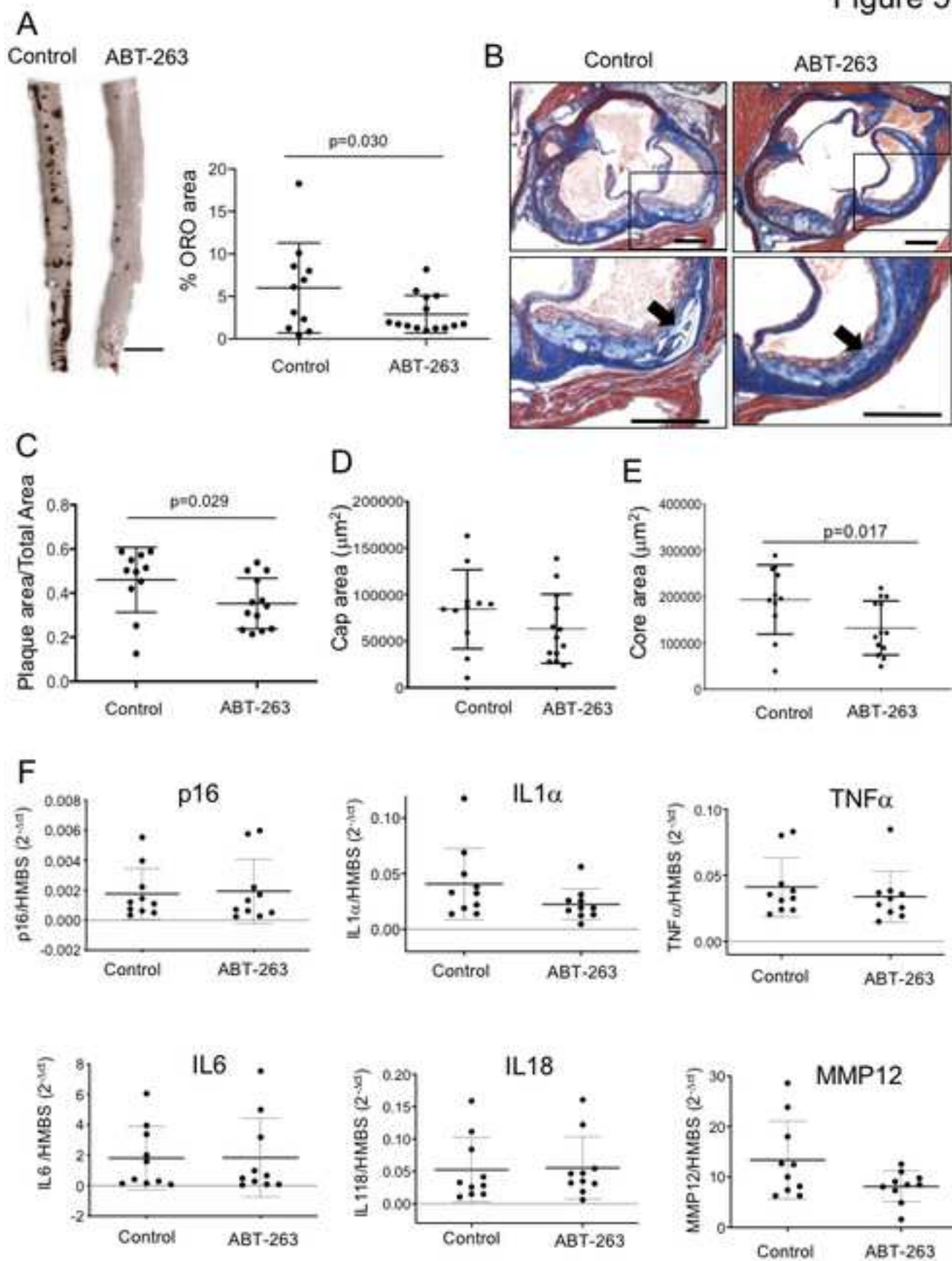
Figure 6
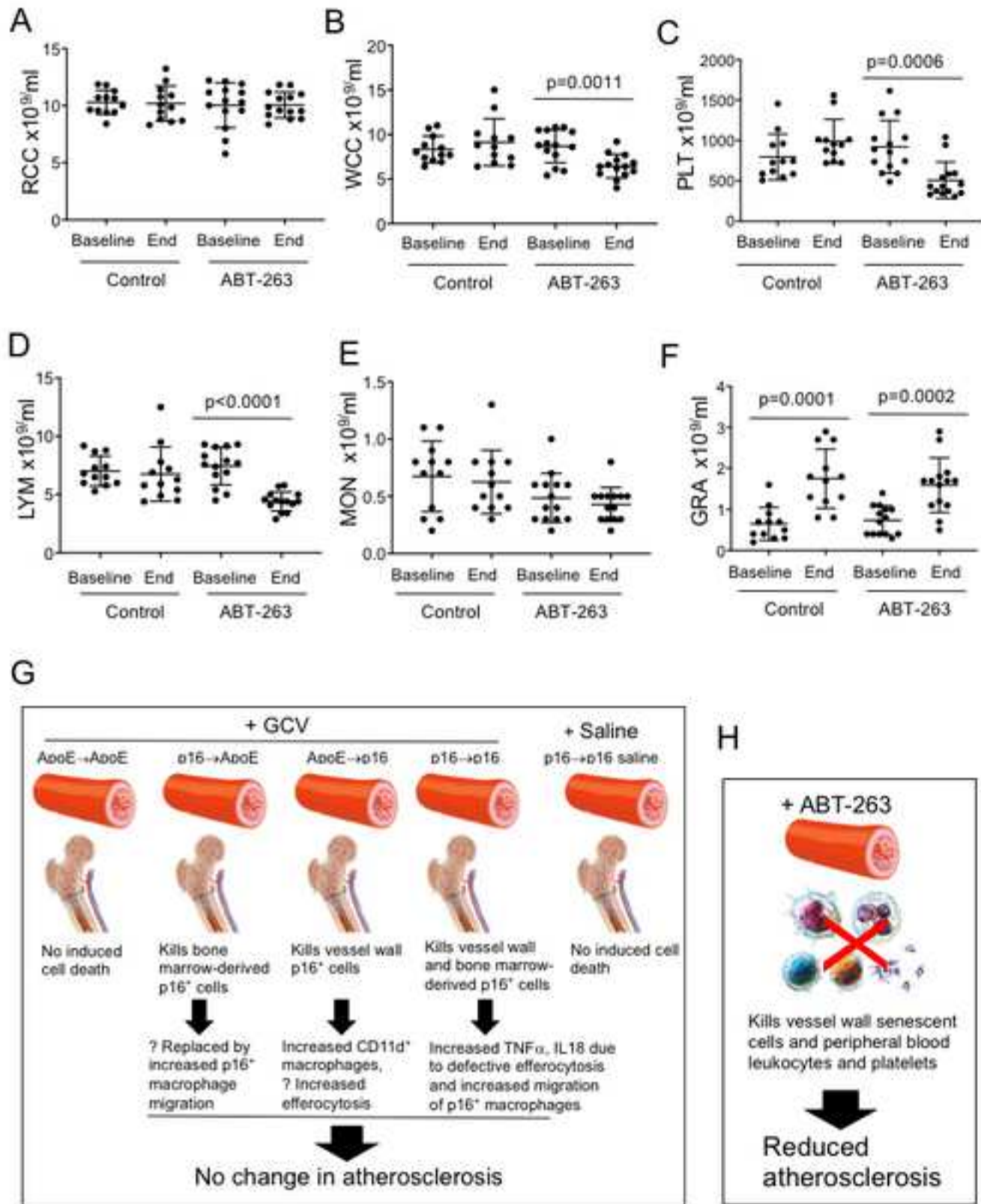
Genetic senolysis
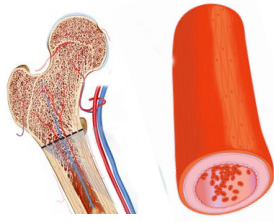
Increased apoptosis,
Inflammation

No change in atherosclerosis

Drug-induced senolysis

Kills peripheral blood leukocytes
and platelets

Reduced atherosclerosis

Graphical Abstract
Effects of p16-induced genetic senolysis or ABT-263 drug-induced senolysis on atherosclerosis.

SUPPLEMENTAL MATERIAL

Efficacy and limitations of senolysis in atherosclerosis

Abel Martin Garrido[1], Anuradha Kaistha[1], Anna K Uryga[1], Sebnem Oc[1], Kirsty Foote[1], Aarti Shah[1], Alison Finigan[1], Nichola Figg[1], Lina Dobnikar[1,2], Helle Jørgensen[1], Martin Bennett[1,*]

[1]Division of Cardiovascular Medicine, University of Cambridge, and [2]Nuclear Dynamics Programme, Babraham Institute, Cambridge UK

<u>**Supplemental Methods**</u>
Isolation of human VSMCs
After removal of the adventitia and endothelium, human aortic VSMCs were isolated using the explant method and cultured in Smooth Muscle Cell Growth Medium 2 (Promocell). After 1 month cells were trypsinized and re-seeded at 13 400 cells/cm^2 for subsequent passages, and then at 3500 cells/cm^2 when cells approached senescence to maintain a similar confluency. Media was replaced every 2-3 days. For Doxorubicin experiments, passage 2 cells were treated with Doxorubicin (250nM, Cayman) or vehicle (DMSO, Sigma-Aldrich) for 24h, washed three times with PBS and incubated with complete fresh media for 21d. For replicative senescence experiments, cells were considered senescent with no increase in cell number and minimal EdU incorporation over 14d.

Isolation of mouse VSMCs
Mouse aortic VSMCs (mVSMCs) were isolated by enzymatic digestion. Briefly, the whole aorta was dissected from 8-12w old mice, cleaned of adventitial fat, and incubated for 10min at 37°C with 1mg/mL Collagenase IV (ThermoFisher Scientific, MA, USA) and 1U/mL Elastase in DMEM (Sigma-Aldrich). The adventitia and endothelium were removed, the aortas cut into explants and incubated with 2.5mg/mL Collagenase IV and 2.5U Elastase in DMEM at 37°C to obtain a single cell suspension. Cells were centrifuged at 220g for 5 min at room temperature and the pellet re-suspended in DMEM with 20% FBS. After 1 month, cells were switched to 10% FBS, split 1:2 when confluent and used in exponential growth (<passage 3). mVSMCs were treated with different concentrations of Doxorubicin (Cayman) or DMSO (Sigma-Aldrich) for 24h, washed three times with PBS and incubated in fresh complete media for 7d.

Isolation of mouse bone marrow-derived macrophages
Bone marrow-derived macrophages (BMDM) were isolated by removal of femurs and tibias from 8-10w old mice, bone marrow flushed in RPMI media and filtered through a 40μm cell strainer (Corning). Cells were centrifuged at 300g for 10 min, and re-suspended at 2 x10^6 cells/ml in complete RPMI (RPMI with 20% FBS) + 15% L929 conditional media in a non-tissue culture dish. Cells for assays at different time points were seeded at the same initial density, and CD11b and CD115 expression were assayed by flow cytometry after 7d to verify purity. mRNA and protein were isolated at 7, 21 and 28d. Macrophages differentiated for 7d were detached using accutase, counted and were re-plated at 4.2x10^4 cells/cm^2 in tissue culture plates.

qPCR
mRNA was isolated using Nucleospin RNA columns (Macherey-Nagel, Düren, Germany) and concentrations determined by Nanodrop. cDNA was synthesized using Quantitect Reverse Transcription Kit (Qiagen, UK) using 1 μg of mRNA or Omniscript RT Kit (Qiagen, UK) using 500ng mRNA. All primers are listed in **Supplemental Table 3.** Forward and reverse primers were used at 10mM final concentration, and a Rotorgene SYBR Green RT-PCR Kit (Qiagen, UK) used. PCR conditions were: 5 min 95°C, and 40 cycles of (10s at 95°C followed by annealing/extension at 60°C for 30s), and a melting curve performed at the end of the reaction. Expression Master Mix (ThermoFisher Scientific, MA, USA) was used with a final concentration of 1X probe/primers for quantification of mRNA levels using Taqman. The PCR conditions were: 10 min at 95°C and 40 cycles of (15s at 95°C followed by 1 min at 60°C). Each gene gave a single peak and its product size was verified on an agarose gel. Taqman probe efficiencies were 0.93-0.99 based on a standard curve with serial dilutions of the template for each set of primers. Gene expression was calculated using delta Ct ($2^{-\Delta Ct}$) or delta-delta Ct ($2^{-\Delta\Delta Ct}$) against housekeeping genes (GAPDH for human and RPL4/HMBS for mouse).

EdU incorporation

EdU assays were performed using the Click-iT™ Plus EdU Cell Proliferation Kit for Imaging, Alexa Fluor™ 647 dye (ThermoFisher Scientific, MA, USA) following the manufacturer's recommendations. Briefly, cells on glass coverslips were incubated with EdU (10uM) for 24 hours, fixed in 4% formaldehyde for 15 min and permeabilized in 0.5% Triton for 30 min. Cells were incubated with Alexa Fluor® picolyl azide 647 for 30 min to stain EdU$^+$ cells. Finally, samples were counterstained with DAPI to analyze total cell number and Pro-Long Diamond (ThermoFisher Scientific Ma, USA) was used as an antifade mountant. Cells were analyzed using Leica TCS SP5 confocal laser scanning microscope at 20X and EdU$^+$ and total cells were quantified manually using LAS AF (Leica Application Suite Advanced Fluorescence) software.

SAβG activity

SAβG activity in vitro was assessed using the Senescence Cells Histochemical Staining kit (Sigma-Aldrich) following the manufacturer's recommendations. Briefly, 4×10^4 cells were plated in 12-well plate a day prior to staining. The next day, cells were fixed with 1x fixation buffer for 7 min. at RT, washed and then incubated with staining mixture at 37^0C overnight. Images were clicked using Nikon TMS-F microscope with GXCAM LITE live camera and quantified using ImageJ software.

Western blots

Proteins were separated by SDS-PAGE, and wet transferred to a 0.22 μm pore (p16^{Ink4a} and p21) or 0.45 μm pore PVDF membrane (Millipore) (other proteins). After blocking for 1h at room temperature in 0.1% TBS-T in 5% non-fat milk, membranes were incubated with primary antibody overnight at 4$^°$C in 0.1% TBS-T in 5% non-fat milk. Membranes were washed 3 times with 0.1% TBS-T, and incubated with a secondary-linked HRP antibody for 1h at room temperature in 0.1% TBS-T in 5% non-fat milk. Membranes were washed 3 times for 10 min with 0.1% TBS-T and chemiluminescence detected using Amersham ECL detection reagents (Amersham). Primary/secondary antibodies used for Western blot are listed in **Supplemental Table 4**.

p16-3MR mice

p16-3MR mice were a kind gift from Professor Judith Campisi (Buck Institute, CA) and were genotyped using a specific Taqman probe against RLuc (see below), that allowed quantification between homozygous or heterozygous p16-3MR mice. Briefly, 60ng of genomic DNA (gDNA) was isolated from ear notches and qPCR performed for RFP or Luciferase using a Taqman probe against GAPDH that can recognise gDNA as a loading control. Mice were anaesthetized with inhaled isofluorane (2.5% in 1.5 L min^{-1} O$_2$; maintained at 1.5%). Animals were sacrificed by CO$_2$ inhalation with subsequent rapid snap-freezing of tissue.

Immunohistochemistry

Paraffin-embedded and formalin fixed sections (5 μm) were deparaffinised and rehydrated through graded ethanol solutions to water. Atherosclerotic extent and composition was determined with Masson's trichrome (HT15 kit, sigma Aldrich) staining. Briefly, sections were preheated in Bouin's solution at 56 ºC for 15 minutes, cooled and cleaned in tap water to remove yellow colour and then Stained in working Weigert's Iron Haematoxylin solution for 5 minutes. Sections were again washed in water, rinsed in deionised water and Stained in Biebrich Scarlet Acid Fucshin for 5 minutes. Following rinsing in deionised water, sections were placed in working posphotungstic/Phosphomolybdic Acid solution, then in Aniline Blue solution for 5 minutes each. Sections were then placed in 1% Acetic Acid for 1 minute, rinsed, dehydrated through alcohol, cleared in xylene and mounted.

For Mac-3 immunohistochemical analysis, de-waxed and rehydrated sections were cooked in 120 mM sodium citrate buffer and endogenous peroxidase activity was blocked with 3% hydrogen peroxide. After blocking in 10% BSA sections were immunostained overnight for

MAC3 (1:400, BD Pharmingen 553322). Next day, HRP-conjugated secondary antibody was applied (anti Rat 1:300, Vector BA4001) and visualized using DAB (DAB vector SK 4105). For TUNEL assay, Incorporation of dUTPdigoxigenin was detected with an alkaline phosphatase-conjugated antibody to digoxigenin (Roche) and development with 5-bromo-4-chloro-3indoyl-phosphate/p-nitroblue tetrazolium (Vector). Three random fields of each slide were chosen using a bright-field microscope with imaging software (Image-Pro Insight 9.1 Media Cybernetics, MD, USA). Positive cells were counted using ImageJ software (NIH, MD, USA). Percent positive cells was calculated by dividing positively stained cells by total number of cells. The average of percentage in three fields was then taken as the final percentage of positive cells for each slide.

In vivo bioluminescence imaging

p16-3MR mice were irradiated with a dose of 9 Gy followed by bone marrow transplant (12 million bone marrow cells in 200 uL) from p16-3MR mice donors. After 4 months, mice were injected with 150 µL of RediJect Coelenterazine H Bioluminescent Substrate (150ug/mL, Perkin Elmer) intraperitoneally. After 15 minutes, mice were anaesthetized by isofluorane and placed in a NightOWLII Analyzer (Berthold Technologies). Luminescence was measured for 5 min at 37°C 25 min post injection, setting the x- and y- bins to 8 with high gain and slow read out using IndiGO software (Berthold Technologies).
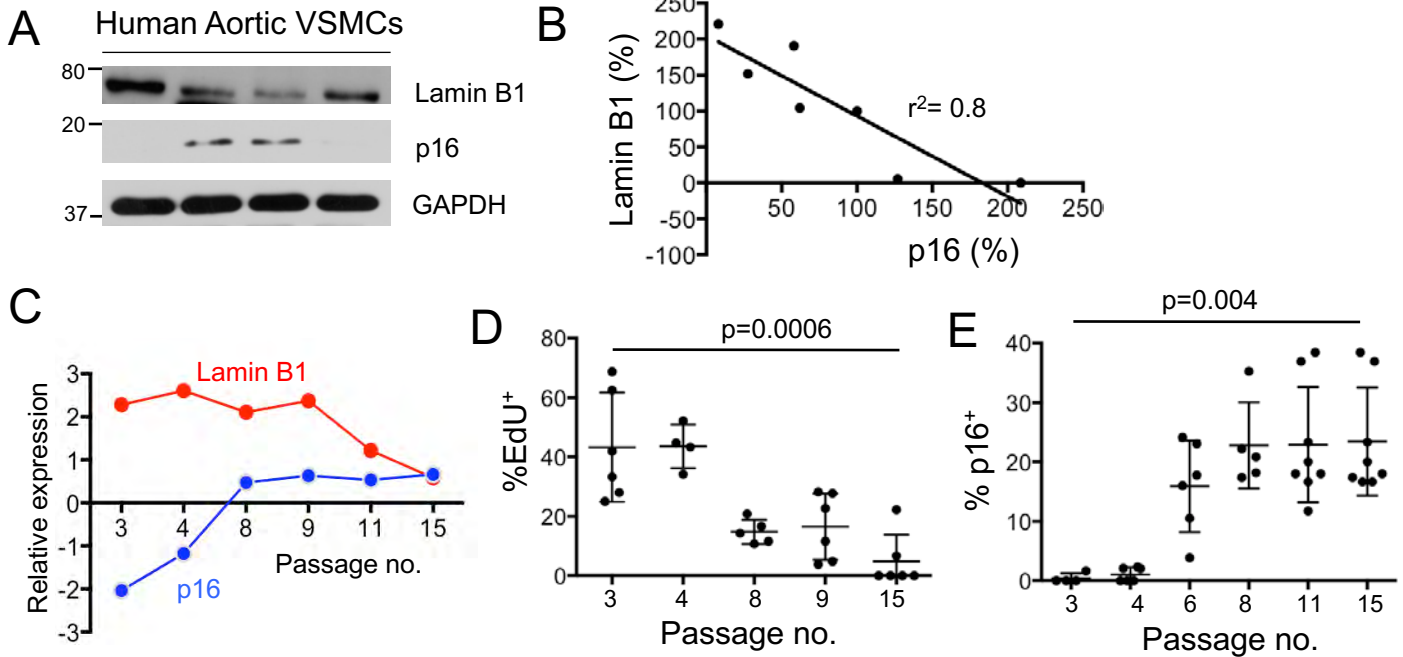
Supplemental Figure 1.
(A) Representative Western blot for Lamin B1 and p16 in 4 different primary human VSMC isolates. **(B)** Expression of Lamin B1 and p16 protein relative to GAPDH for 7 different primary human VSMC isolates. **(C)** qPCR of p16 and Lamin B1 mRNA expression relative to housekeeping genes in human aortic VSMCs with increasing culture passage. **(D-E)** %EdU$^+$ **(D)** or %p16$^+$ **(E)** cells in 4-6 different human primary VSMC cell cultures according to cell passage. Data are means (SD), Kruskal-Wallis test **(D-E)**.
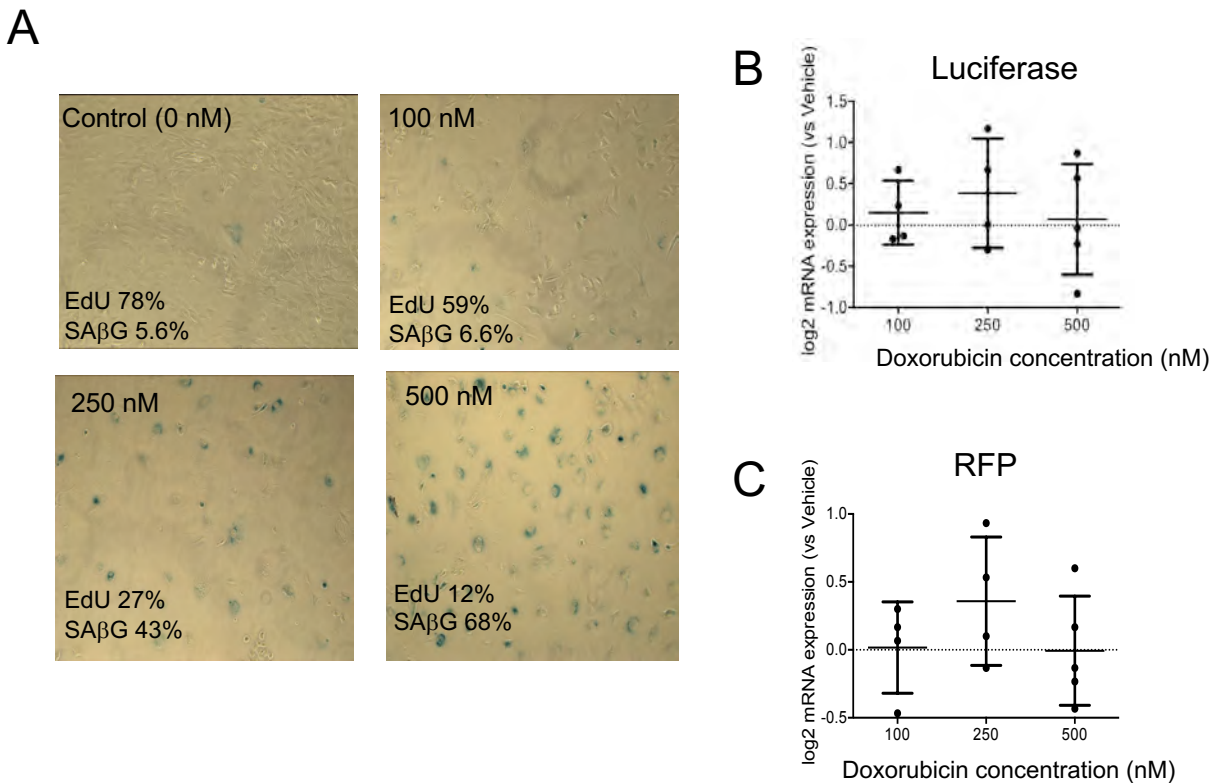
Supplemental Figure 2.
(A) Photomicrographs of mouse VSMCs stained for SAβG after treatment with vehicle control or increasing concentrations of doxorubicin for 1d and isolated after an additional 7d. **(B-C)** qPCR for Luciferase or RFP mRNA expression relative to GAPDH in mouse p16-3MR VSMCs treated with increasing concentrations of doxorubicin for 1d vs. vehicle control followed by 7d recovery. Data are means (SD) n=4-5. Mann Whitney U test.
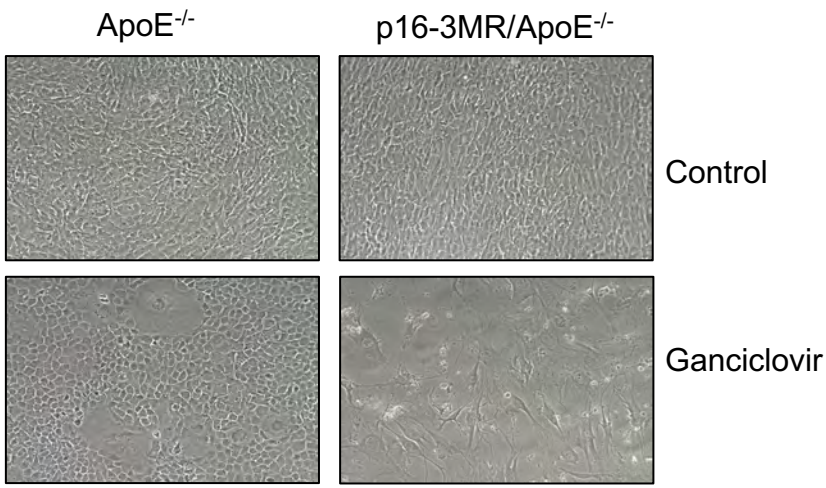
Supplemental Figure 3.
Phase-contrast micrographs of cell cultures of ApoE$^{-/-}$ or p16-3MR/ApoE$^{-/-}$ VSMCs incubated for 6d with vehicle control or Ganciclovir (10µg/mL).
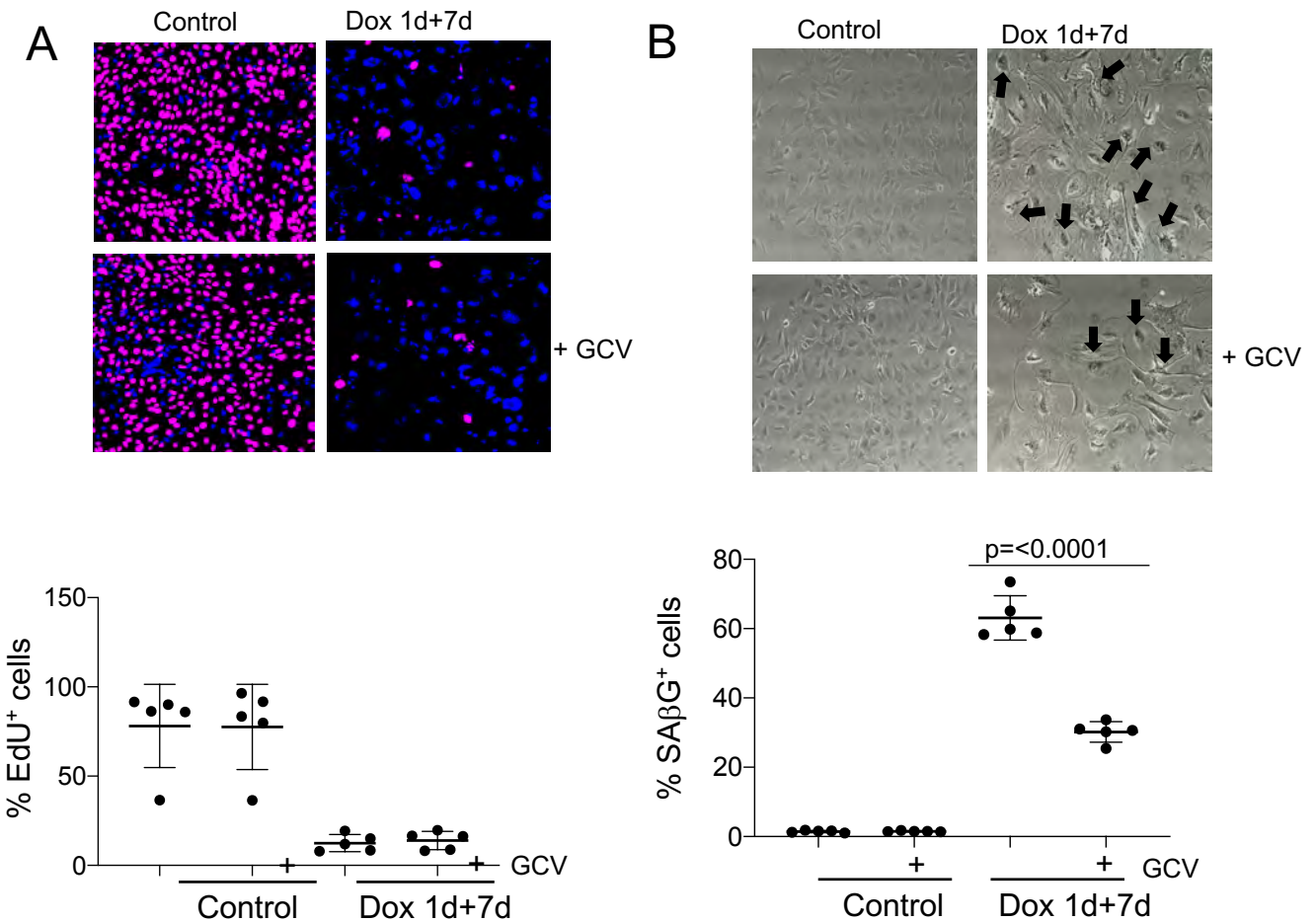
Supplemental Figure 4.
(A-B) Control mouse p16-3MR VSMCs or after 500nM Dox1d treatment +7d recovery, each group ± 1µM GCV treatment for 48h stained for EdU **(A)** or SAβG **(B)**. Arrows indicate SAβG$^+$ cells. Data are means (SD), Mann Whitney U test **(A)**, Unpaired student t-test **(B)**. n=5.
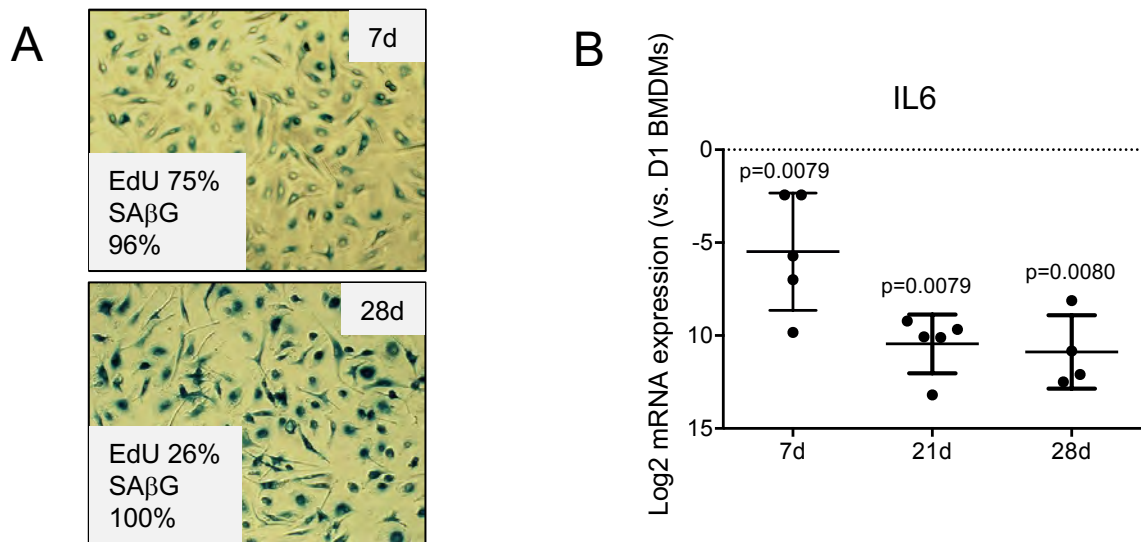
Supplemental Figure 5.
(A). Phase contrast micrographs of mouse macrophages stained for SAβG at 7d and 28d of culture. **(B)** qPCR for relative IL6 mRNA expression in mouse macrophages at 7d, 21d and 28d of culture vs. D1 bone marrow-derived macrophages (BMDMs). Data are means (SD), n=4-5. Mann Whitney U test.
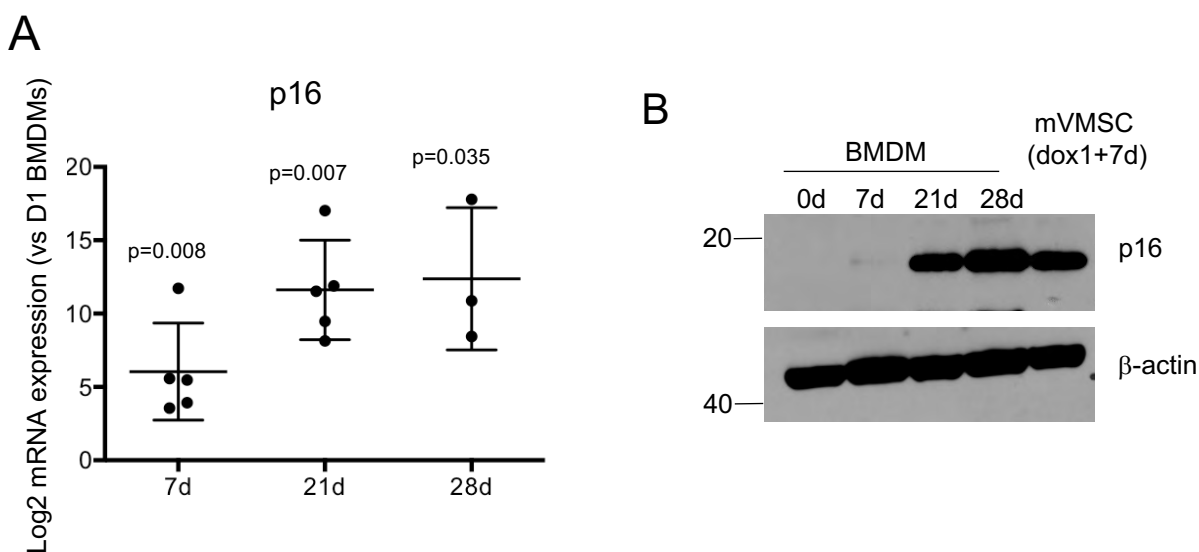
Supplemental Figure 6.
(A) qPCR for p16 mRNA expression in mouse p16-3MR macrophages at 7-28d in culture vs. day 1 BMDMs. Data are means (SD). (n=3-5). Mann Whitney U test. **(B)** Western blot for p16 of mouse p16-3MR macrophages at 7-28d vs mouse VSMCs treated with Dox 1+7d.
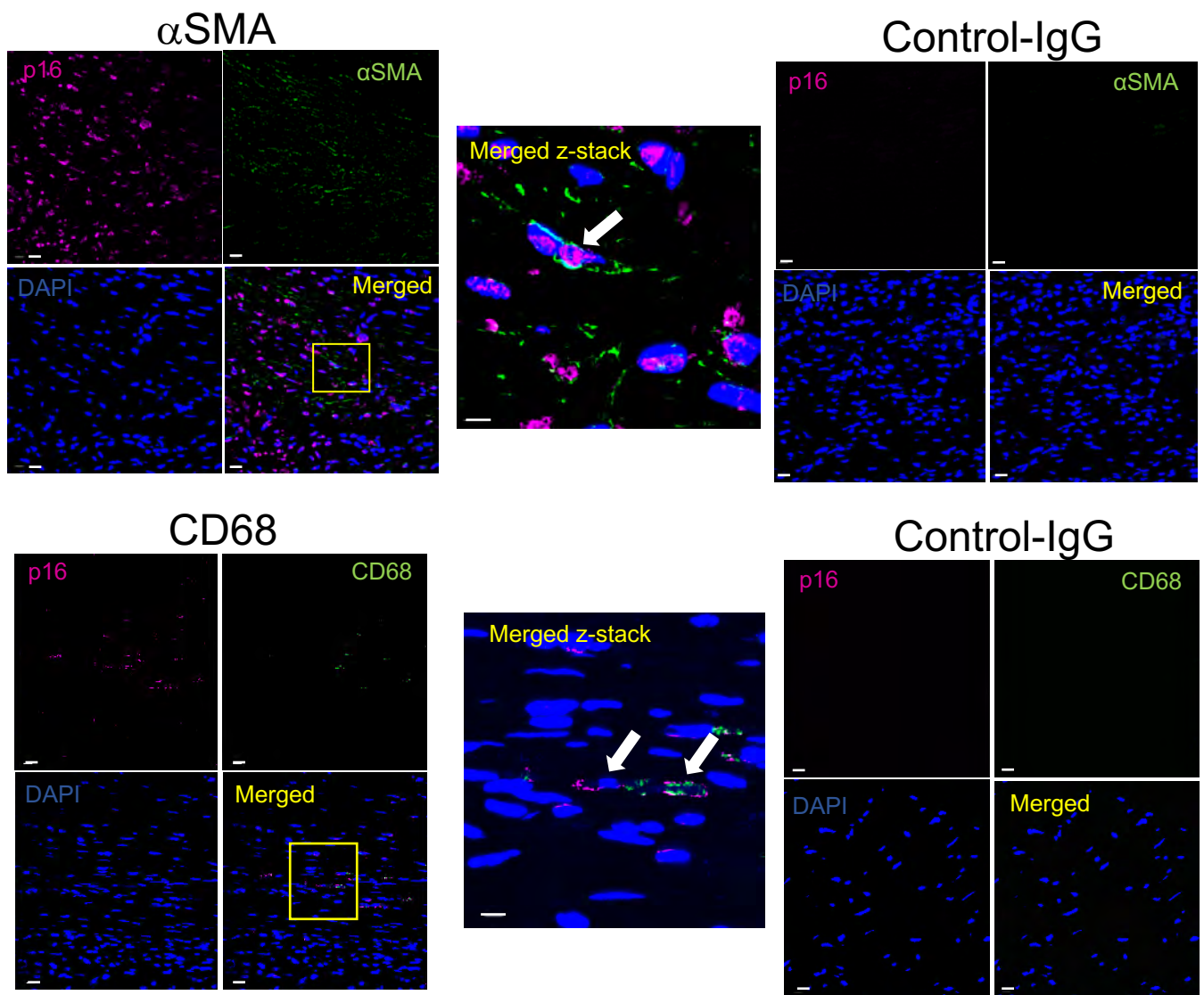
Supplemental Figure 7.
Confocal microscopic images of human carotid plaques for p16 co-labeled with αSMA or CD68 or their isotype negative controls and DAPI. Scale bars =10μm in sequential images and 5μm in Z-stack. Arrows indicate p16+/αSMA+ or p16+/CD68+ cells. n=4 human plaques.
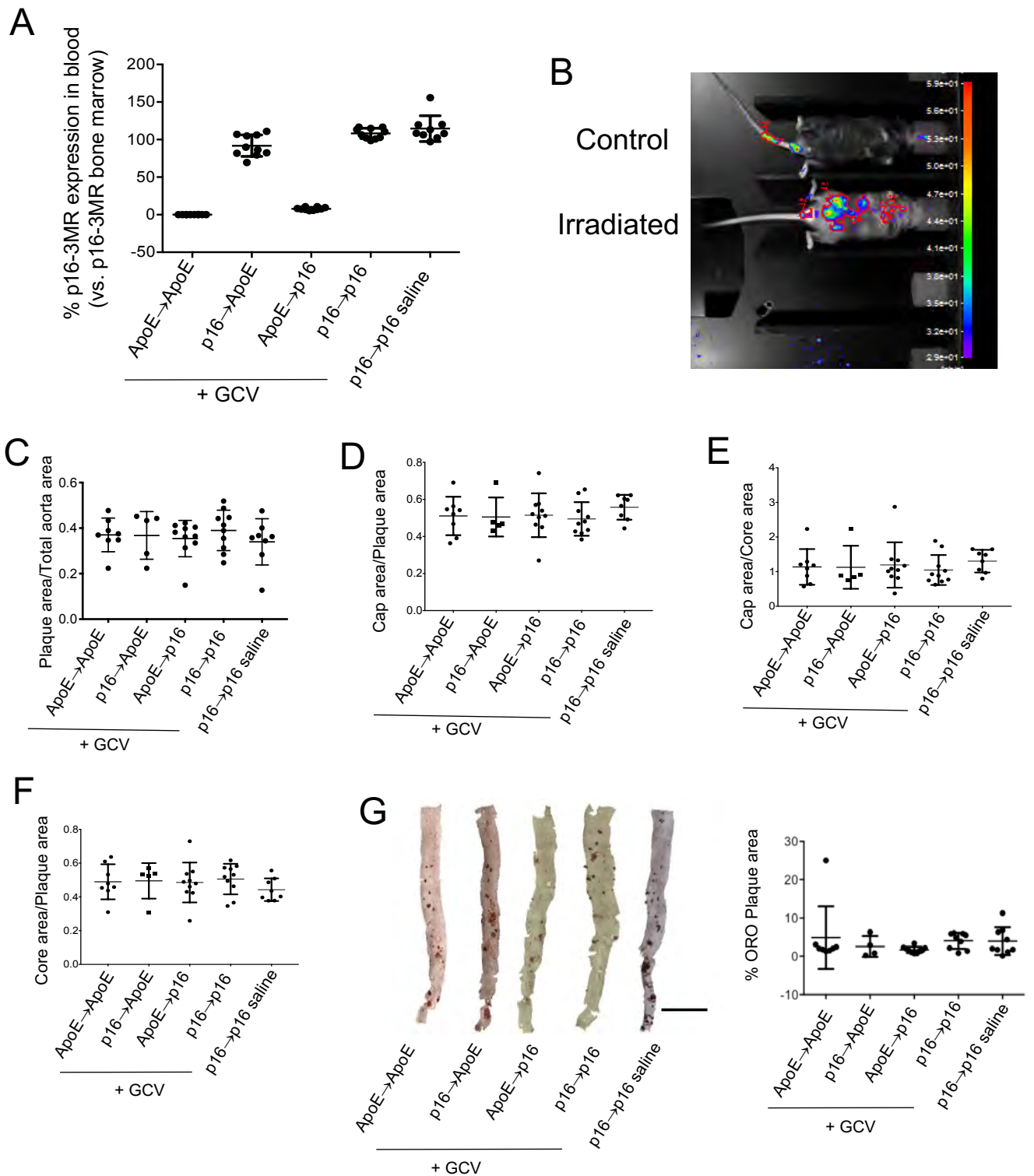
Supplemental Figure 8.
(A) qPCR for p16-3MR expression in blood of experimental mice compared with p16-3MR bone marrow.
(B) Bioluminescence of control p16-3MR mice or 3m after 9Gy irradiation. **(C-F)** Plaque/Total area, Cap area/plaque area, Cap area/Core area, and Core area/Plaque area for aortic roots of experimental mice**.** n=5-10. **(G)** ORO staining of mouse descending aorta in experimental mice and quantification of %ORO area. Scale bar = 3mm. Data are means (SD), n=4-10. 1-way ANOVA with correction for multiple comparisons.
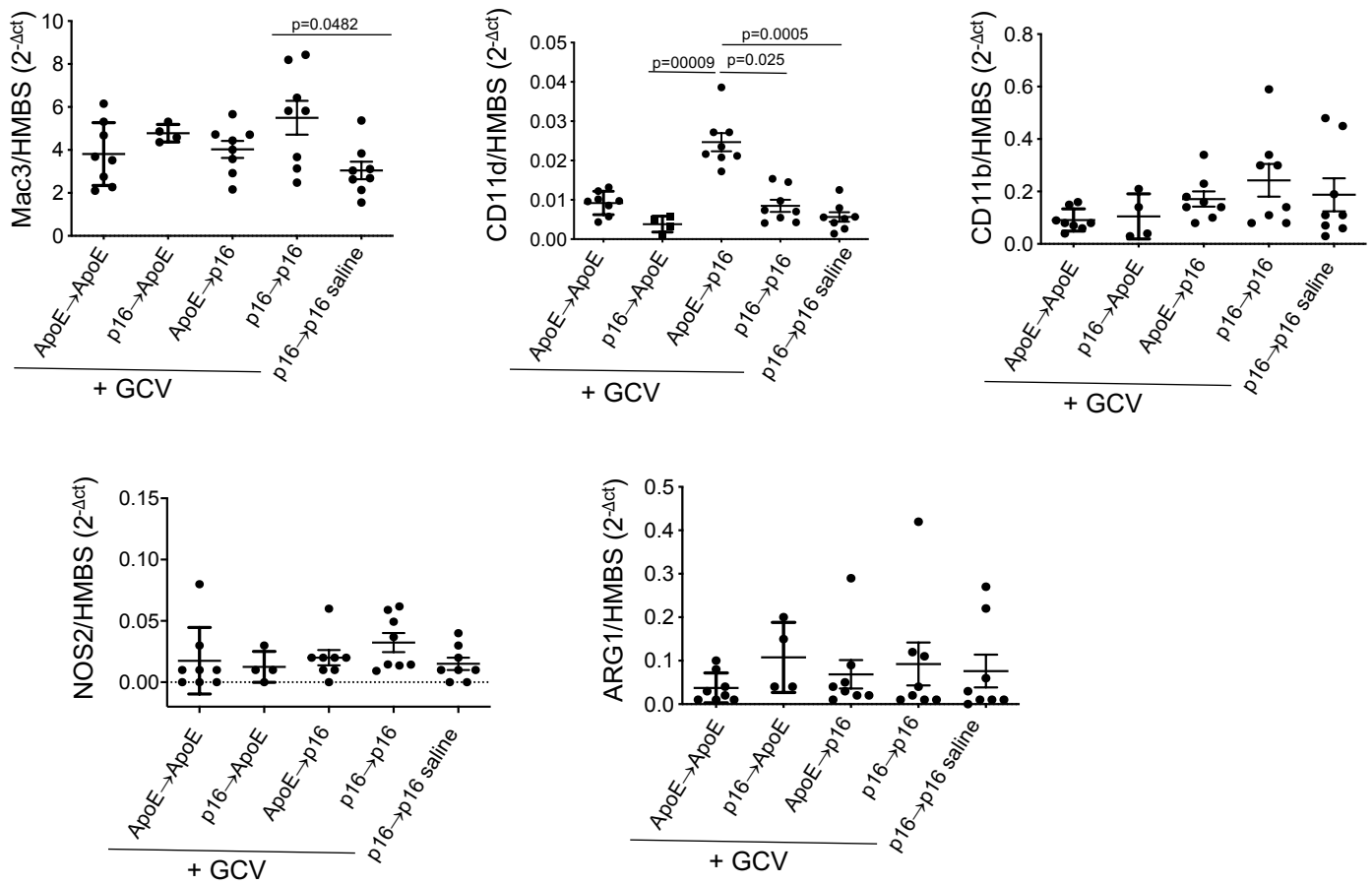
Supplemental Figure 9.
Relative mRNA expression for Mac3, CD11d, CD11b, NOS2 or ARG1 in experimental mice. Data are means (SD) n=5-10 mice. Kruskal-Wallis H Test followed by Dunn's multiple comparisons test.

A

B
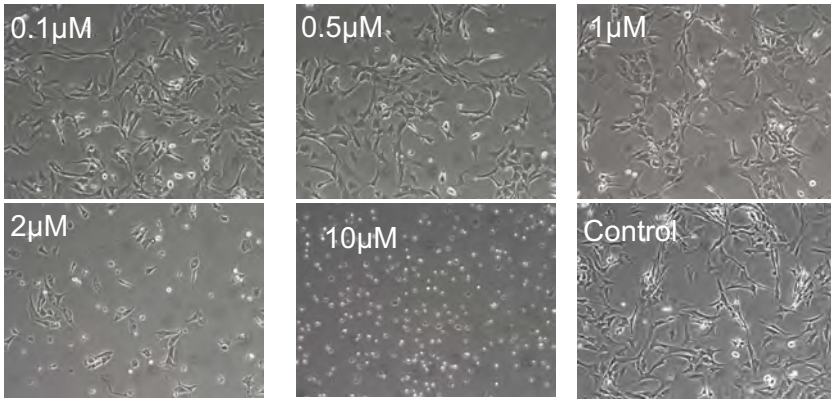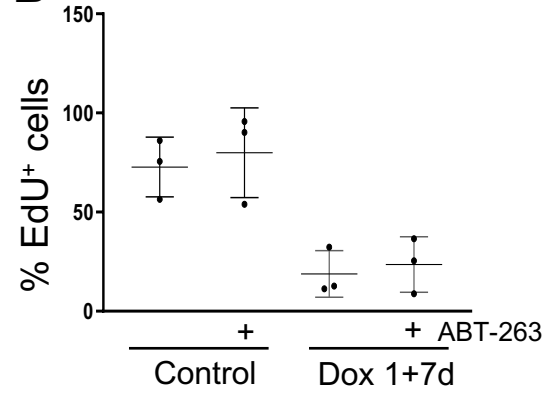
Supplemental Figure 10.
(A) Photomicrographs of proliferating mouse VSMCs after treatment for 48h with increasing concentrations of ABT-263. **(B)** % EdU+ of replicating control mouse VSMCs or after Dox1d treatment +7d recovery, or each group ± 1μM ABT-263 treatment for 48h. Data are means (SD), n=3. Unpaired student t-test.
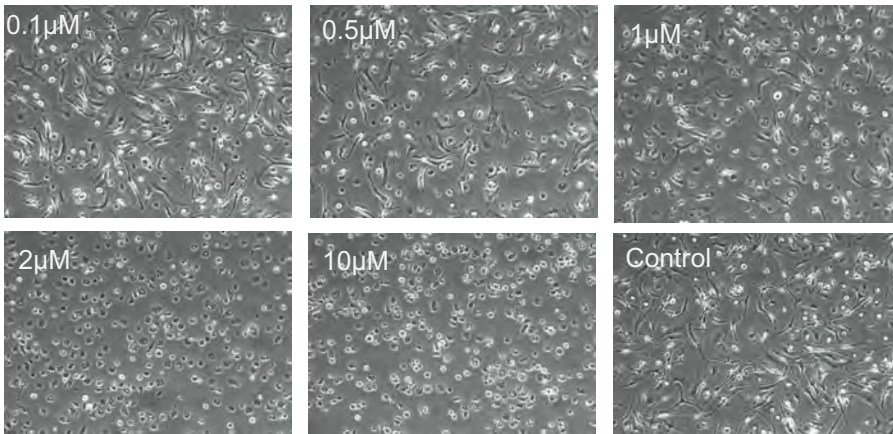
Supplemental Figure 11.
Photomicrographs of mouse macrophages cultured for 28d, and then treated with control or increasing concentrations of ABT-263 for 48h.
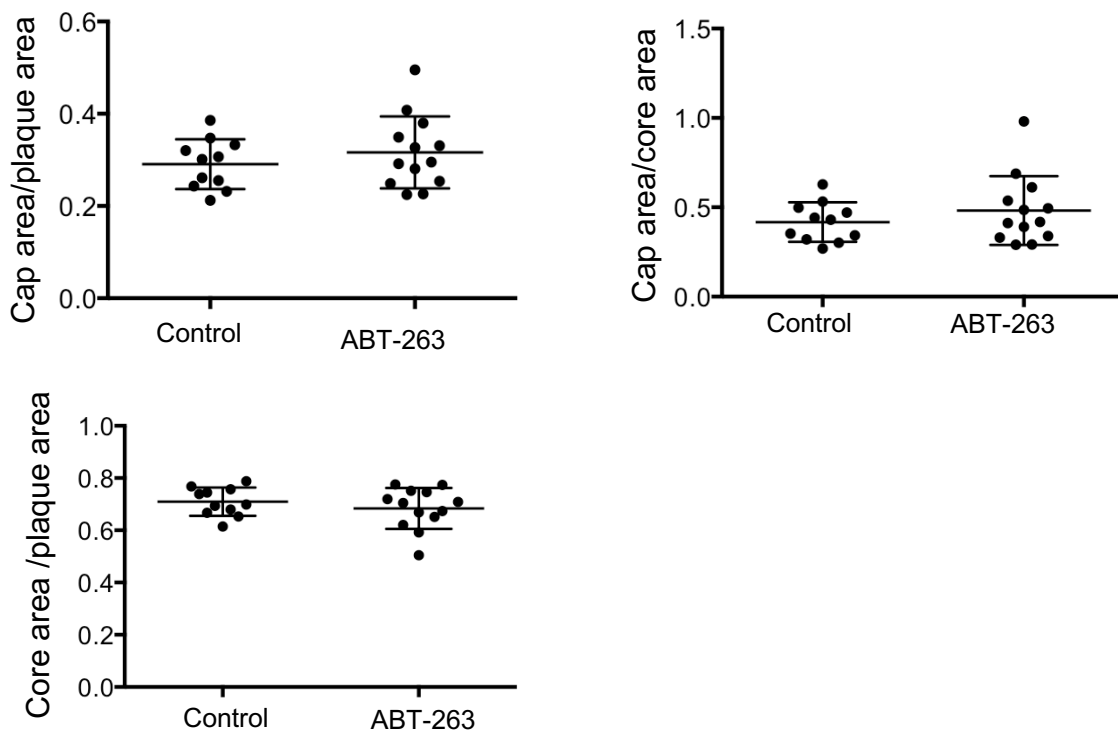
Supplemental Figure 12.
Cap area/Plaque area, Cap area/Core area or Core area/Plaque area for mouse aortic root atherosclerotic plaques from mice treated with control or ABT-263. Data are means (SD), n=11-13. Unpaired Student t-test.

A

B
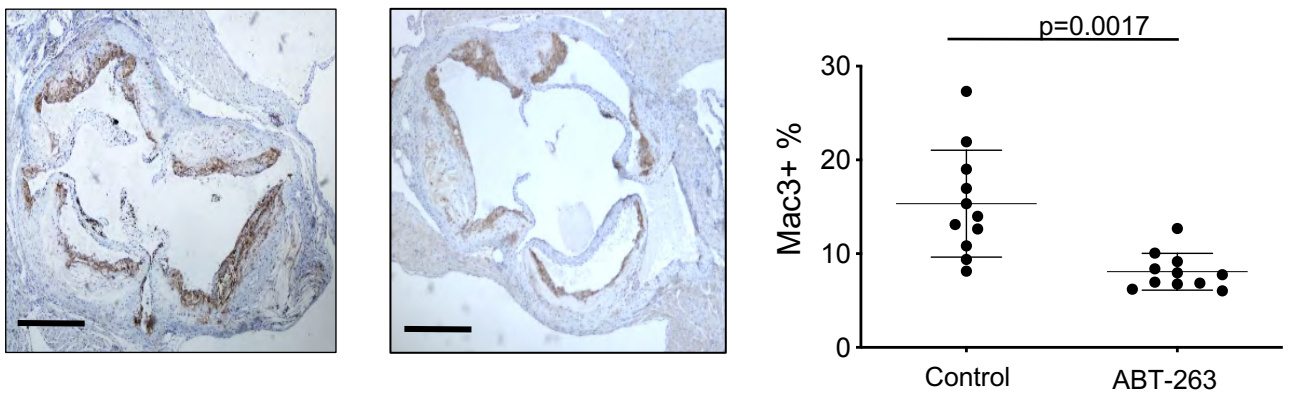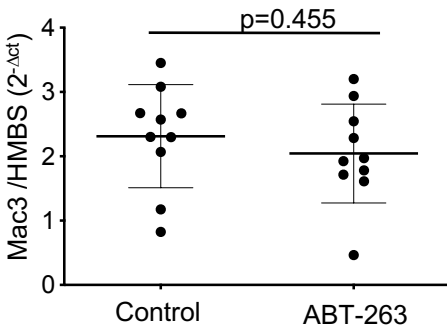
Supplemental Figure 13.
(A) Immunohistochemistry for mac3 and quantification for mouse aortic root atherosclerotic plaques from mice treated with control or ABT-263**.** Scale bar=300μm**. (B)** qPCR for relative expression of Mac3 in aortic arches of experimental mice against the housekeeping gene HMBS. Data are means (SD), n=11, Welch's t-test **(A)** or n=10,Unpaired Student t test**(B)**

GCV

	ApoE→ApoE	p16→ApoE	ApoE→p16	p16→p16	p16→p16 saline
Lipids (mmol/L)					
Cholesterol	14.66 (5.7)	16.9 (2.4)	15.35 (4.8)	19.33 (2.6)	15.83 (5.9)
LDL	13.51(5.5)	15.63 (2.45)	14.17 (4.4)	17.80 (2.3)	14.94 (5.9)
HDL	0.45 (0.13)	0.52 (0.16)	0.59 (0.23)	0.81(0.36)	0.55 (0.34)
Triglycerides	1.51 (0.48)	1.67 (0.41)	1.30 (0.52)	1.62 (0.55)	1.35 (0.68)
Cytokines (pg/ml)					
TNFα	25.91(9.2)	38.80(20.2)	18.54 (7.5)	21.77 (7.7)	31.44 (18.7)
IFN-γ	0.65 (0.26)	1.10 (0.78)	1.10 (0.49)	0.8 (0.33)	0.82 (0.47)
IL1β	1.97 (0.95)	1.60 (0.62)	1.84 (0.50)	1.56 (0.73)	1.30 (0.19)
IL2	3.66 (1.1)	3.42 (0.64)	3.45 (1.30)	2.69 (1.37)	2.53 (0.68)
IL5	4.37 (2.2)	6.73 (2.1)	5.68 (2.8)	14.37 (23.4)	10.62 (11.4)
IL6	202.8 (220)	189.6 (155.2)	60.48 (43.4)	54.80 (42.3)	69.36 (39.0)
IL10	55.80 (27.7)	55.10 (19.2)	42.1 (8.3)	30.84 (12.6)	37.00 (11.24)
CXCL1	138.5 (113.2)	112.4 (8.7)	92.76 (29.9)	145.8 (53.5)	148.9 (46.7)

Supplemental Table 1
Serum lipids and cytokines of ApoE→ApoE, p16→ApoE, ApoE→p16, or p16→p16 mice + GCV, or p16→p16 mice + saline. Data are means (SD), n=5-10. 1-way ANOVA with corrections for multiple comparisons

	Control	ABT-263	Statistical analysis (p value)
Lipids (mmol/L)			
Cholesterol	16.24 (3.9)	17.36 (3.4)	0.44
LDL	15.08 (3.7)	16.16 (3.3)	0.43
HDL	0.37 (0.1)	0.35 (0.1)	0.80
Triglycerides	1.80 (0.7)	1.84 (0.6)	0.87
Cytokines (pg/ml)			
TNFα	23.92 (6.7)	22.14 (8.1)	0.55
IFN-γ	1.38 (1.5)	0.90 (0.4)	0.25
IL1β	2.02 (1.1)	1.80 (1.0)	0.61
MCP1	46.42 (15.0)	61.07 (27.4)	0.11
IL5	7.68 (5.0)	6.59 (2.7)	0.49
IL6	**138.8 (116.3)**	**45.36 (21.5)**	**0.007**
IL10	38.58 (11.3)	35.71 (12.4)	0.55
KC/GRO	72.50 (18.9)	64.43 (29.8)	0.43

Supplemental Table 2

Serum lipids and cytokines of ApoE$^{-/-}$ mice treated with control or ABT-263. Data are means (SD). n=12-14. Unpaired Student t-test.

Human

Gene	Forward 5'-3'	Reverse 5'-3'
p16 INK4a	CCAACGCACCGAATAGTTACG	GCGCTGCCCATCATCATG
ACTA2	AGACCCTGTTCCAGCCATC	TGCTAGGGCCGTGATCTC
Commercial	**Company**	**Reference**
p21	Qiagen	QT00062090
LmnB1	Thermo	Hs01059210_m1
GAPDH	Thermo	Hs02786624_g1

Mouse

Gene	Forward 5'-3'	Reverse 5'-3'
LMB1	GGGAAGTTTATTCGCTTGAAGA	ATCTCCCAGCCTCCCATT
IL6	CTCTGCAAGAGACTTCCATCCA	AGTCTCCTCTCCGGACTTGT
p16 Ink4A	TTGAGCAGAAGAGCTGCTACGT	CGTACCCCGATTCAGGTGAT
p21	GCAGATCCACAGCGATATCC	CAACTGCTCACTGTCCACGG
RLUC	TCCAGATTGTCCGCAACTAC	CTTCTTAGCTCCCTCGACAATAG
mRFP1	GAAGGGCGAGATCAAGATGA	GACCTCGGCGTCGTAGTG
F4/80	CTTTGGCTATGGGCTTCCAGTC	GGAGGACAGAGTTTATCGTG
ACTA2	GTCCCAGACATCAGGGAGTAA	TCGGATACTTCAGCGTCAGGA
RPL4	CGCAACATCCCTGGTATTACT	ACTTCCGGAAAGCACTCTCCG
	CCGTGCTCCTTGTAGACTTAAC	GCCAGAGTAGCTTGTCCTCC
IL1α	TCAACCAAACTATATATCAGGATGTGG	CGAGTAGGCATACATGTCAAATTTTAC
IL18	TCTTGGCCCAGGAACAATGG	ACAGTGAAGTCGGCCAAAGT
MMP12	TTCATGAACAGCAACAAGGAA	TTGATGGCAAAGGTGGTACA
TNFα	AGGGTCTGGGCCATAGAACT	CAGCCTCTTCTCATTCCTGC
HMBS	ACTGGTGGAGTATGGAGTCTCAGATGGC	GCCAGGCTGATGCCCAGGTT
Commercial	**Company**	**Reference**
GAPDH	Thermo	Mm99999915_g1

Mouse (Taqman)

Gene	Forward 5'-3'	Reverse 5'-3'	Probe 5'-3'
RLUC	TCCAGATTGTCCGCAACTAC	CTTCTTAGCTCCCTCGACAATAG	FAM-CCAGCGACGATCTGCCTAAGATGTT-MGB
mRFP1	GAAGGGCGAGATCAAGATGA	GACCTCGGCGTCGTAGTG	Universal probe 161 (Roche)

Supplemental Table 3
Synthesised or commercial primers used for human and mouse qPCR

Human

Antibody	Reactivity	Company	Catalog number	Dilution	Secondary
Anti p16^{Ink4a}	Human	ProteinTech	10883-1-AP	1/1000	Rabbit
Anti p21 (12D1)	Human	Cell signalling	#2947	1/1000	Rabbit
Anti GAPDH (14C10)	Human	Cell signalling	#2118	1/1000	Rabbit
Anti LmnB1 (M-20)	Human	Santa Cruz	No longer available	1/250	Goat
Anti p53 (DO-7)	Human	Cell signalling	#48818	1/1000	Mouse
Secondary					
Anti Rabbit		Cell signaling	#7074	1/1000	
Anti Mouse		Amersham	LNA931V/AG	1/1000	
Anti Goat		Santa Cruz	sc-2354	1/1000	

Mouse

Antibody	Reactivity	Company	Catalog number	Dilution	Secondary
Anti p16^{Ink4a}	Mouse	Abcam	ab211542	1/1000	Rabbit
Anti p16^{Ink4a}	Mouse	Gift		1/500	Rat
Anti LmnB1 (M-20)	Mouse	Santa Cruz	No longer available	1/250	Goat
p21	Mouse	Santa Cruz	No longer available	1/100	Rabbit
Anti α/β tubulin	Mouse		#2148	1/3000	Rabbit
Secondary					
Anti Rabbit		Cell signalling	#7074	1/1000	
Anti Mouse		Amersham	LNA931V/AG	1/1000	
Anti Goat		Santa Cruz	sc-2354	1/1000	
Anti Rat		Amersham	NA935V	1/1000	

Supplemental Table 4
Primary and secondary antibodies used for Western blotting. An anti-mouse p16 antibody was also generously provided by Dr Manuel Serrano, Institute for Research in Biomedicine, Barcelona.